MODELING OF VARIABLE ENERGY RESOURCES IN POWER SYSTEM RELIABILITY ASSESSMENT

By

Samer Sulaeman

A DISSERTATION

Submitted to
Michigan State University
in partial fulfillment of the requirements
for the degree of

Electrical Engineering-Doctor of Philosophy

2017

ABSTRACT

MODELING OF VARIABLE ENERGY RESOURCES IN POWER SYSTEM RELIABILITY ASSESSMENT

By

Samer Sulaeman

In recent years, the reliability evaluation of power systems has been receiving increasing attention. This is largely because of the ongoing changes in generation portfolios and environmental constraints. In the assessment of the increasing penetration levels of variable energy resources (VERs), such as wind turbine generators (WTGs) and photovoltaic (PV) systems, reliability methods associated with improved modeling and related phenomena have an essential role. One important factor the planning of wind power and PV systems projects is to measure the contribution of such resources to the adequacy of the power system. For power systems, the intermittent nature of VERs introduces a new level of complexity of modeling such resources using traditional reliability methods used for conventional generators. In contrast to conventional generators, VERs differ in terms of capability and dispatchability. Also, the fuel source of VERs cannot always be made available and controlled. This is due to the fact that the outputs of VERs depend mainly upon the availability of the input (wind or solar irradiation), and their outputs show a high degree of correlation. Therefore, the output of individual generators in the same farm cannot be modeled independently in the probabilistic reliability studies. The work presented in thesis develops an analytical method to model the output of large wind farms and PV systems for power system reliability assessment. Further, a reliability model of VERs that can be used for power system reliability assessment including VERs is developed. The solution of the aforementioned problems is addressed in this work by separately modeling the independent mechanical failures of gener-

ation units and the dependency on the input, and then convolving the two distributions. The resulting model includes both probability and frequency distributions of the power output of the VERs. The proposed method reduces the complexity of modeling the VERs, as it considers the effects of input dependency, correlation, and system component failures on reliability assessment. The resulting model is used to evaluate the reliability of test systems in the presence of VERs in several case studies. In power system adequacy assessment, capacity value is used to measure the contribution of VERs to the overall system adequacy. Iterative methods are traditionally used to calculate the capacity value of VERs. However, iterative methods are computationally demanding, especially for large systems. In this work, a direct, non-iterative method is developed to calculate the capacity value of VERs while considering the effect of the input uncertainty and the failure of generation units. The method developed in this work is based on augmenting the cumulative distribution function (CDF) of the generation margin (prior to adding VERs) to include the output power of VERs. From the augmented CDF of the generation margin, the capacity value is analytically determined without performing iterations. The presented method reduces modeling complexity and the computational burden associated with calculating the capacity value of VERs.

My Mother, wife and my four little children

ACKNOWLEDGMENTS

First and foremost, I would like to express my sincerest and deepest appreciation to my advisor, Professor Joydeep Mitra. It has been an honor to be his Ph.D. student. He has taught me and inspired me, both consciously and unconsciously, how to be a part of a research team. Notably, for creating the research environment in which I have performed my graduate studies. I appreciate his contributions of time, ideas and interminable support to make my Ph.D. experience productive and stimulating. The joy and enthusiasm he has for his research group was contagious and motivational for me, even during tough times in the Ph.D. pursuit. I am greatly fortunate to have him as my advisor and mentor.

I would also like to thank Professor Subir Biswas, Professor Fang Z. Peng, Professor Shlomo Levental and Professor Jongeun Choi for serving on my committee and their valuable suggestions and comments. A word of gratitude goes to Professor Tim Hogan and Professor Kalyanmoy Deb for their support to complete my work. I would like to thank Dr. Mohammed Ben-Idris for his contribution, comments, suggestions, and collaboration.

I sincerely acknowledge the funding sources that helped me to complete my Ph.D. work: the Libyan North American Program and the Ministry of Higher Education and Scientific Research-Libya, and the Electrical and Computer Engineering Department at Michigan State University. I would also like to thank my friends at Michigan State University and the research group at the ERISE lab.

Most of all, I appreciate the support and encouragement of my family: my mother, my wife, and my sisters.

TABLE OF CONTENTS

LIST OF TABLES

LIST OF FIGURES

Chapter 1

Introduction

In recent years, the drive to bring about technological and regulatory changes that concern energy, natural resources and climate change has gathered significant momentum. Out of the numerous changes that the power grid is undergoing, perhaps the most transformative is the inclusion of VERs such as wind and photovoltaic (PV) systems. Despite their numerous advantages, the inclusion of variable energy resources (VERs) in the steady-state analysis of power systems such as power system reliability assessment, for instance, has also brought up a number of technological and operational issues that need to be addressed. The input uncertainty and the output fluctuation of VERs bring concerns into the power system planning and operation especially with increasing VERs penetration levels. In response to the growing need for a proper method to model the output of VERs with high accuracy and reduction of modeling complexity of VERs in power system reliability assessment, the work reported in this thesis develops a reliability model of VERs for power system reliability studies.

1.1 Motivation

In response to the rapid growth of the global economy, environmental concerns, economic incentives of fossil fueled generating units, and global warming awareness, the movement towards renewable energy resources has gained significant momentum. Despite the advantages of such resources, the new reality of input uncertainty and output fluctuation has introduced another layer of complexity to the planning and operation of power systems. From a reliability point of view, the major problem and barrier to effectively utilizing the intermittent resources is the fact that they are intermittent and stochastic in nature. For instance, a wind farm comprises a multitude of wind turbine generators (WTGs) spread out over a geographic area. The operating characteristics of wind turbines differ from those of traditional power plants in terms of their capability and dispatchability. Moreover, in a wind farm, all wind turbines are driven by the same input (wind). Output depends upon the variable input and output correlation of wind turbines, which increases modeling complexity. In addition to the dependency on the input and the correlation between generation units, failure of WTGs adds more challenges and complexity to the application of reliability assessment methods that are applicable to conventional generators.

The grid-connected PV systems are constructed from a large number of components such as power electronic circuits and solar panels. The functionality of such components is highly dependent upon the operating and ambient conditions. The operating conditions and environmental factors may lead to an overall reduction in output power and the failure of system components. Given the large number of components involved in PV systems and the intermittency of the source (solar), modeling of these systems in reliability evaluation studies is a complex task due to the dependency of output power on an intermittent source (solar) and the availability of a large number of system components. In addition, in a PV farm, PV panels are placed adjacent to each other, and all PV panels will be subjected to the same solar radiation and experience approximately the same operational and environmental factors that may affect the output of the farm. Failure of wind farm generation units and PV systems have a significant impact on available power. Several studies show that the operation and environmental factors could lead to different failure modes of VERs [1–8]. In addition, when input is not available, generators would be unavailable to generate power. The effect of input shortage in this case can be regarded as forced outage rates, which are much higher when considering the intermittency of the input. In general, Mote Carlo simulation is usually adopted for a reliability model of variable energy resources, Mote Carlo simulation able to capture a wide range of modeling detail and system dependencies. However, Mote Carlo simulation becomes time consuming, especially when implemented in a large and complex system. Further, solution accuracy depends mainly on the number of sampling performed. The purpose of this research is to construct a model for a cluster of output power for wind farms and PV systems. For power system adequacy assessment, Monte Carlo simulation is normally not considered appropriate for model building. A direct analytical method is considered a better approach for building reliability models. This work develop a model that combines a cluster of variable resources into a single equivalent multi-state unit that captures their correlation, output variability, and forced outages that can be incorporated into traditional probabilistic planning methods without further regard to the correlation between generating units within the farm.

1.2 Challenges

The challenges that were addressed in this thesis are summarized as follows:

A. One of the challenges imposed by the increasing penetration of wind generation and PV systems is how to model the output power of such resources, considering the operational characteristics and failures of generation units.

B. The intermittent nature and uncertainty of variable energy resources introduces complexity to applying traditional reliability methods applied to conventional generators.

C. The operating characteristics of variable energy resources differ from those of traditional power plants in terms of their capability and dispatchability.

D. Variable energy resources are contracted over a geographic area in the form of farms. These farms comprise a multitude of generation units (wind turbines or PV panels) spread out over a geographic area, and their output shows correlation. Therefore, the output of individual units cannot be modeled as independent random variables.

E. For a wind farm, the output power of wind turbines in a particular geographical location is highly dependent on the wind speed regime at that particular site. In addition, wind speed experiences variation all the time, and the dependency on geographical location and seasonality increases the complexity of providing a generalized model that describes the correlation between wind turbines output at a wind farm location.

F. Capacity value is used as a measure of the capacity contribution of intermittent resources in power system capacity planning. An evaluation process in this case is carried out to make sure that the system reliability will be maintained when the VERs are introduced to the power grid. The input variability, failure of VERs, and correlation is a matter of modeling complexity in evaluating the capacity value of VERs. Therefore, in the assessment of such resources in the traditional effective load carrying capability calculation method, the output of a wind farm or PV system is considered a load modifier. The capacity credit in this case may not be realistically represented.

G. Iterative methods are traditionally used to calculate the capacity value of VERs. However, iterative methods are computationally expensive and time consuming, especially for large and complex systems. Therefore, developing a direct, non-iterative method that considers the effect of the input intermittency, forced outages of VERs, and correlation of the output of VERs with system load would present a more computationally efficient alternative to the system planner.

H. Although the integration of wind power has several advantages, it poses several technical challenges such as variability and uncertainty of wind speed and failures of wind turbine generators (WTGs) which may deteriorate the reliability of power systems. One of the most practical solutions to mitigate these drawbacks is the use of energy storage systems. However, variability and uncertainty of wind speed and failures of WTGs not only deteriorate the reliability of power system but also complicate the process of determining suitable sizes of energy storage systems for a specific reliability target.

1.3 Organization of the Thesis

The remainder of this thesis is organized as follows: Chapter 2 presents a literature review of the methods used in power system adequacy assessment in presence of VERs. Chapter 3 discuses the reliability method used for power system adequacy assessment. Chapter 4 presents the development of an analytical method to model the outputs of VERs in power system adequacy assessment. Chapter 5 discuses the reliability methods used for calculating the capacity value of VERs and presents the development of a new method to calculate the capacity value of VERs. Chapter 6 presents an implementation of an analytical approach to quantify the size of energy storage to firm up wind power. Chapter 7 summaries the findings and provides a general conclusion about the methods that have been developed in this work.

Chapter 2

Background and Literature Review

2.1 Modeling the Output of Wind Farms in Power System Adequacy

The reliability assessment of systems that integrate wind power and associated technical aspects such as adequacy assessment and the determination of wind farm capacity values has been amply addressed in the literature [9–14]. In [15] a discrete state algorithm is adopted to model the reliability of unconventional energy resources. The hourly modified generation model of unconventional generators based on their generation capacity is combined with conventional generators to determine the hourly loss of load expectation and the frequency of capacity deficiency. In [16], load and wind are treated as correlated random variables. Monte Carlo simulation is used to evaluate system reliability. The time correlation between load and wind power is considered in the clustering process by assigning for each load value a specific value of wind power that occurs in the same time-frame.

Several methods have been proposed for analytical reliability modeling of wind farms to include the effect of forced outages of WTGs. For instance, a multi-state capacity outage probability model has been proposed in [17]. However, the frequency and duration indices in power system reliability assessment cannot be calculated using this model. A more comprehensive model that takes into account frequency and duration indices has been proposed in [18]. This model combines the wind speed model and the WTG reliability model using a multi-layer concept. In this model, the wind speed is classified into a finite number of states, and WTGs are modeled as two states, *up* and *down*. A birth-death Markov chain is used to model wind speed transitions. However, in reality, wind speed transitions cannot be assumed to transit smoothly to the next neighboring state through the birth-death process unless the sampling time is close to zero. Therefore, if the model is to be used for wind speed, some transitions between wind speed will be lost, and the steady state probabilities will not be correct. Also, two failure rates (corresponding to normal and extreme wind speeds) for WTGs are considered, which require duplicating the model although the effect of failures due to extreme wind speeds is very low, as concluded in [18]. In fact, if extreme wind speeds are considered higher than the cut-out speed of WTGs, these wind speeds correspond to zero output power, regardless of whether or not the state of the WTGs is up or down. Therefore, the computation burden can be significantly reduced if forced outages of WTGs due to extreme wind speeds are aggregated with the state of zero output power. Further, for a wind farm consisting of n wind speed states and m wind turbines, there will be $(2^m * n)$ possible states. Therefore, for large wind farms, the size of the full Markov matrix would be extremely large. This adds a complexity to the modeling process and computation burden due to the large number of system states [14, 19–21].

A method to determine an equivalent capacity of wind farms based on Monte Carlo simulation is presented in [22]. Monte Carlo simulation has also been used to evaluate the reliability indices of wind power in [23–25]. Although Monte Carlo simulation can be used for the evaluation of complex systems, analytical methods using system data and characteristics are considered more suited for the construction of reliability models. However, the purpose of this research is to build a model for a cluster of wind turbines, a direct analytical method is considered to offer a better approach for building reliability models. In this work, therefore, Monte Carlo simulation is only used for model validation.

2.2 Modeling the Output of PV Systems in Power System Adequacy

In the literature, most of the work presented on the reliability aspects of PV systems has examined the performance of the major power electronic components and circuits, such as capacitors, IGBTs, or the entire inverter, to assess the reliability of PV systems [26–28]. The power electronic circuits deliver the output power of PV panels to the load or to the main grid. Reliability assessment of the power electronic circuits of grid-connected PV systems for different typologies have been addressed in the literature [29–31]. In the evaluation process, the mean time to failure (MTTF) has been used as an indicator for system reliability; the overall reliability of a circuit has been calculated by summing the failure rates (the failure rate is the reciprocal of the MTTF) of the components [32–34]. However, this is true only if the failure of a component leads to an overall failure of the power electronic circuit. In some cases such as multilevel inverters, a redundancy exists in power electronic topologies and their desired function is not totally affected by a component failure [35, 36]. The Monte Carlo simulation technique has been used in [37] for reliability assessment of a hybrid system of wind and PV systems. A combination of deterministic and probabilistic techniques has been used in the reliability evaluation of these systems. In [38], the hourly mean solar radiation data has been used as the main input and a Monte Carlo simulation technique was implemented to evaluate system reliability. In [39], an analytical method has been used to model the availability of the PV systems in the reliability assessment. In [40], reliability of a wind and solar system has been evaluated using Monte Carlo simulation technique. In [41], a methodology for PV system reliability and economic analysis has been introduced. The proposed method is used to model the reliability of a PV system that could be utilized to estimate life-cycle energy costs.

Grid-connected PV systems are constructed from a large number of components, including power electronic circuits and solar panels. The performance of such components is highly dependent upon their operation and ambient conditions. Operational and environmental factors may lead to an overall reduction in the output power and the failure of system components [42,43]. Given the large number of components involved in PV systems and the intermittency of the source (solar), the modeling of these systems in reliability studies is a complex task. From the reliability point of view, the output model of PV systems should be able to capture the effect of the input variability and the failures of system components.

2.3 Capacity Value

Capacity value is used as a quantitative measure to determine the capacity of conventional units that can be replaced by renewable generation, which enhances system reliability or at least provides the same reliability target prior to adding these resources to the system. In determining the capacity value of variable energy resources, the effective load carrying capability (ELCC) approach has been favorably used among the available criteria [44]. The ELCC approach is based on calculating the amount of load increase that would result in reliability indices equal to system indices prior to adding the VERs. The common practice of the existing methods is the use of the reliability indices such as the LOLE (loss of load expectation) index as a criterion to determine the capacity value of VERs; other reliability indices such as the LOLF (loss of load frequency) index are rarely considered. In addition, the impact of forced outages of wind farm generating units on the output is usually ignored.

Several methods have been introduced in the literature to calculate the capacity value of VERs [44–47]. These methods can be classified into intelligent search methods [48], simulation methods [49–57], and analytical methods [58–63]. Further, these methods can be classified into iterative methods [48–60] and non-iterative methods [61–63]. Calculation of the capacity value of VERs based on iterative methods is deemed to be computationally intensive due to the requirement of repetitive calculations. On the other hand, non-iterative methods are direct and computationally efficient; however, some approximations are usually involved. For instance, the method presented in [61] uses a graphical method that is based on the work presented in [64] to estimate the capacity value of wind power. The graphical method is based on approximating the change in the LOLE index versus load increase using an exponential function. Although the graphical method is computationally efficient, this approximation could lead to considerable errors [63]. The method presented in [62], the Z-method, uses the probability distribution of the generation margin to calculate the capacity value of VERs. However, this method assumes that the probability distribution of the generation margin preserves its shape even after adding wind power [65]. Also, the methods presented in [61,62] ignore the correlation between demand and wind power [65]. The non-iterative analytical method presented in [63] uses the concept of joint probability distribution to calculate the ELCC and the capacity value of VERs considering the correlation between the load and the available output power of VERs. However, this method requires a pre-specified value for the LOLE index to be used to calculate the ELCC before and after adding VERs. Further, the accuracy of estimating the ELCC of the system relies on the chosen number of the "coincidental demand-generation levels," whose optimal value is difficult to determine, as the authors have concluded [63].

Iterative methods are commonly used to calculate the capacity value of VERs. However, iterative methods are computationally expensive and time consuming especially for large and complex systems. In addition, determining the optimum sizes of VERs in terms of their capacity values, has not been given much attention; using iterative methods would be extremely complex and computationally expensive as they require several runs for every candidate-installed capacity. Therefore, developing a direct and non-iterative method that considers the effect of the input intermittency, forced outages of VERs generation units, and correlation of the output of VERs with the system load would reduce the computation burden and enable the planner to determine optimum penetration levels of VERs.

2.4 Sizing the Energy Storage

The integration of energy storage systems with intermittent sources has become a practical solution for overcoming these challenges, largely because of the rapid growth in deployment and improved technology of energy storage systems.

In the literature, several authors have discussed the economic aspects of energy storage systems in the electricity market [66–68]. In [69], dynamic programming with time-shift is used to determine the optimal size of battery storage in utility load-leveling operations applied to the Kansas City Power and Light system. The results showed that the optimal size of battery storage varied with the daily and seasonal load variations. Reference [70] uses Benders decomposition to determine the optimal location and size of a compressed air energy storage system. The optimal size of the energy storage is evaluated based on the capital investment in the energy storage system that leads to daily operating cost reductions.

Also, according to [70], the trade-off between the capital cost of the energy storage and the daily system operating cost becomes insignificant as the energy storage investment increases. This can be attributed in part to the high variation of wind power and the high cost and limited operating lifespan of energy storage systems [67, 71, 72]. Due to these factors, several management and control systems have been proposed to optimize their operation [73–75]. In [76], a predictive control method is proposed for controlling the charging and discharging of a battery storage system; the authors concluded that the size of the battery storage system needed to mitigate the hourly variation of wind power and achieve minimum operating costs should be around 75% of the nameplate capacity of the wind farm.

In practice, different types and sizes of energy storage systems have been deployed for different applications such as energy management, backup power, load leveling, frequency regulation, voltage support, and grid stabilization [77, 78]. However, large scale adoption and deployment of energy storage technologies is still limited, largely due to the aforementioned factors [72, 79]. In spite of the fact that the increased generation from renewable sources reduces overall generating costs, emissions, and consumption of fossil fuels, the intermittency and uncertainty of the output raise several concerns, including peak load capability and system adequacy [80–85]. Moreover, maintaining the efficiency and reliability of a grid, especially with high penetration of variable generation, has become a challenging task. Several studies have shown that high penetration levels of wind power could significantly affect power system quality and security due to its intermittency [80, 83].

The cost of an energy storage system is a major factor in the planning of energy storage system projects. In the literature, several authors have summarized and discussed the cost of integrating energy storage systems [86–88]. These studies show that the cost of an energy storage system depends on several factors, including energy storage size and the types of technology used. One of the practical and promising solutions to the problem of energy storage sizing was proposed by Mitra [89, 90]. The proposed method in [89, 90] was used to quantify the size of energy storage systems analytically, in terms of both power and energy capacity, to meet a reliability target.

Chapter 3

Models and Methods

3.1 Power System Adequacy Assessment

Power system reliability evaluation is important for studying the current system to identify weak points in the system, determining what enforcement is needed to meet future demand and planning for new reliable power system, i.e., network expansion. Power system reliability assessment is vital to avoid economic and social losses resulting from power outages.

In general, reliability is used to measure the ability of the system to perform its designated functions under the conditions within which it was designed to operate. For power systems, the system reliability assessment is aimed to measure the system ability to deliver electricity to all points of utilization at acceptable standards and in the amount desired. Power system adequacy assessment methods that are used for generation systems can basically be classified into deterministic and probabilistic [91–93], these methods are described in Figure 3.1. The common criterion for generation adequacy assessment using deterministic method, is to set generation margins equal to a fixed percentage of the forecast peak demand and operating generation margins sufficient to supply the most likely contingencies. The disadvantages of these methods are that they do not account for the stochastic events and the forced outages of generating units, and uncertainty in load demand. On the other hand, the assessment of generation system adequacy using probabilistic methods encounter for the stochastic events and the forced outages of generating units, and uncertainty in load demand [91–93].

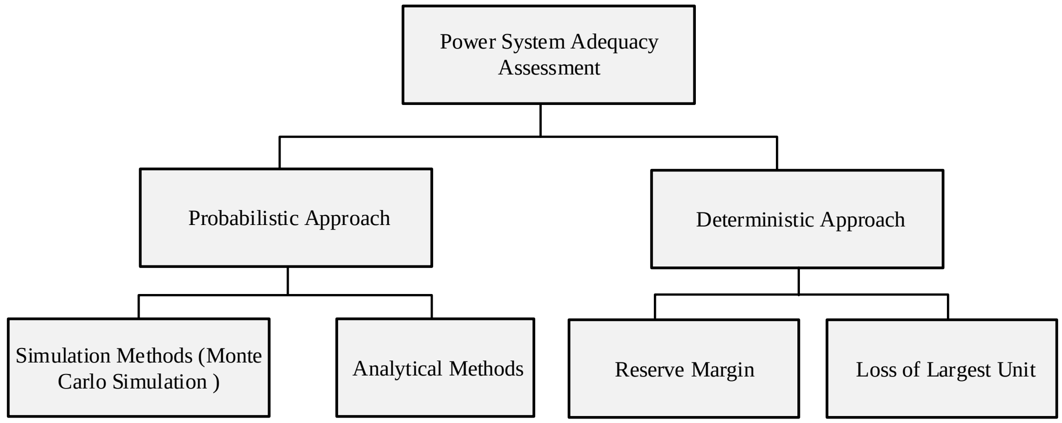

Figure 3.1 Adequacy assessment methods applied for power system

Adequacy assessment methods in power systems are mainly applied to three different hierarchical levels [91, 92]. Due to the complexity of power system, the studies of different hierarchical levels are analyzed separately [91]. At hierarchical level I (HL-I), the total system generation is examined to determine its adequacy to meet the demand. This is usually termed as generating capacity reliability evaluation [91]. In the HL-I studies, the transmission lines are considered highly reliable and able to transfer the generated power to the all load points. On the other hand, in the hierarchical level II (HL-II) studies, the adequacy analysis is usually termed composite system evaluation. HL-II studies can be used to assess the adequacy of an existing or proposed system including the impact of various reinforcement alternatives at both the generation and transmission levels. The objective of the hierarchical level III (HL-III) studies is to obtain suitable adequacy indices at the consumer load points (i.e. distribution level). The hierarchical levels of system adequacy assessment are described in Figure 3.2.

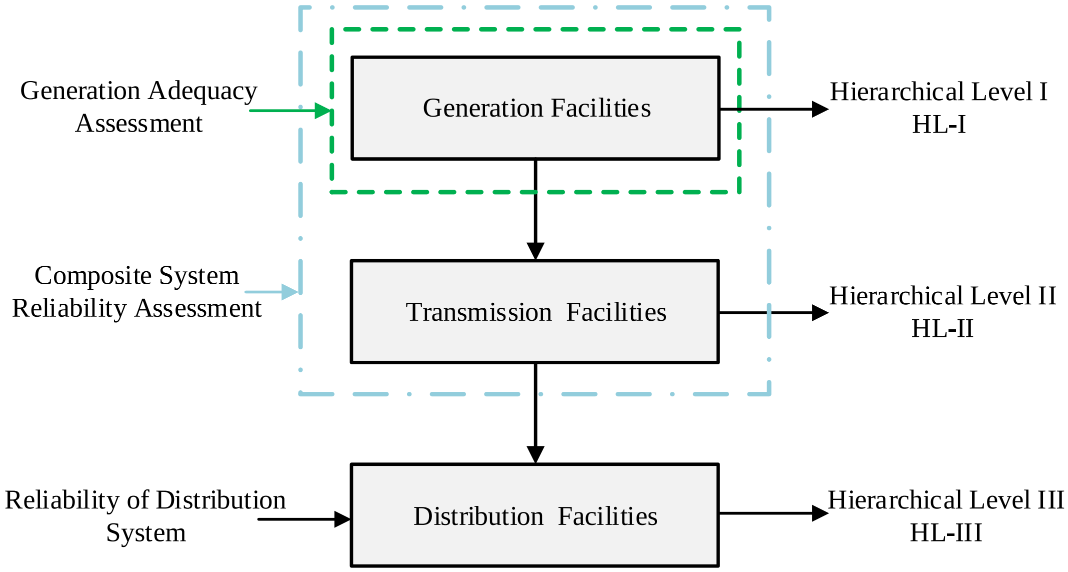

Figure 3.2 Adequacy assessment of power system hierarchical levels

3.2 Analytical Methods

Adequacy analysis of power systems essentially consists of identification and evaluation of failure states, states in which the power system cannot satisfy load demand. According to [91, 92], system adequacy defined as a measure of sufficient facilities within the system to deliver an aggregate electric power and energy requirements without violating system operational constraints. System adequacy is associated with static conditions which do not include system disturbances. The well-known unit addition algorithm is considered a practical method for large-system adequacy analysis. This is a recursive algorithm that starts with the distribution of one unit and successively convolves with it the distributions of the remaining units, one unit at a time. This technique can be used for two-state or multi-state unit and provides a fast technique for building capacity models [93]. Generation adequacy assessment is generally used to evaluate system reliability indices for short-term and long-term generation capacity planning. In this work, the discrete convolution method is used in evaluating the reliability of the system by convolving the discrete probability distributions of generating units to construct a capacity outage probability and frequency table (COPAFT) [93]. In reliability analysis, generation and load models are needed to construct a generation reserve margin of the system from which the reliability indices are calculated.

The reliability assessment using analytical method, the generating system model used for generation capacity adequacy assessment is known as capacity outage probability table and frequency table (COPAFT). In this process, the generation and load models are convolved to form an appropriate risk model where the element of interest is the risk of generation capacity less than the load. In short, adequacy evaluation of generation systems consists of four general steps as shown in Figure 3.3 [91, 92].

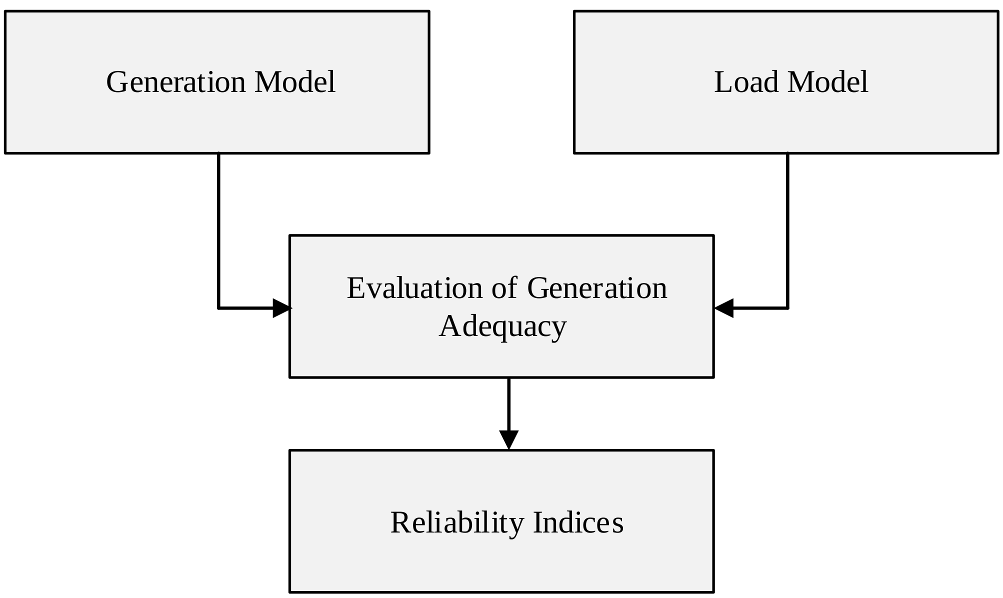

Figure 3.3 Generation reliability evaluation process

3.2.1 Generation Model

For a system composed of N generating units with known forced outage rates (FORs), the COPAFT is built using the *unit addition algorithm*. This is a recursive algorithm that starts with the distribution of one unit and successively convolves it with the distributions of the remaining units, one unit at a time. Considering failures of generating units as independent events, the probability of failure of generation unit can be modeled as Markovian components with two states, *up* and *down* states with known failure and repair rates, λ and μ respectively (λ is the failure transition rate from an up state to a down state, and μ is the repair transition rate from a down state to an up state) as shown in Figure 3.4.

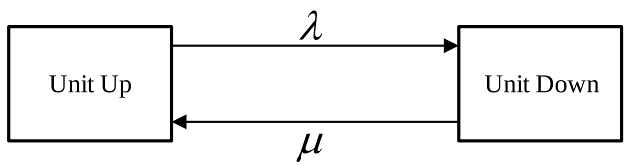

Figure 3.4 Two-state model of a generating unit

Based on the FOR *(forced outage rate is the failure probability)* of generation units, the COPAFT can be built using the unit addition algorithm. This is a recursive algorithm that starts with the distribution of one unit and successively convolves with it the distributions of the remaining units, one unit at a time. The FOR is defined as follows [93].

$$FOR = \frac{\lambda}{\lambda + \mu} = \frac{r}{m + r} \tag{3.1}$$

where m is the mean time to failure ($MTTF$): $MTTF = \frac{1}{\lambda}$, r is the mean time to repair($MTTR$): $MTTR = \frac{1}{\mu}$.

In general, when adding a new unit of capacity C, the cumulative probability and frequency of an outage of X MW can be determined by the following expression: [93, 94].

$$P(X) = \bar{P}(X)(1-q) + \bar{P}(X-C)q, \tag{3.2}$$

where $P(X)$ and $\bar{P}(X)$ denote the cumulative probabilities of the capacity outage state before and after the units are added respectively. Equation (3.2) is initialized as follows.

$$P(X) = \begin{cases} 1, & \text{if } X \leq 0 \\ 0, & \text{otherwise,} \end{cases}$$

The cumulative probability $P(X)$ for a forced outage of X MW or greater can be in general calculated using (3.3).

$$P(X) = \sum_i P(X_i), \quad \forall\, X_i \leq X, \tag{3.3}$$

where

$$\bar{P}(X) = 1, \quad \forall\, X \leq C,$$

In the case of multi-state generating units, (3.2) can be modified as follows.

$$P(X) = \sum_i^n P(i) \times \bar{P}(X - C_i). \tag{3.4}$$

The cumulative frequency of capacity outage of X MW can also be calculated using the same approach using (3.5).

$$F(X) = F_i\,(1-q) + F_j q + (P_j - P_i) q\mu, \tag{3.5}$$

where q and μ are respectively the probability of failure and repair rate of the new added unit; P_i, P_j, F_i, and F_j are determined from the old COPAFT (prior to adding the new unit); i is the index of the existing capacity outage state, $C_i = X$, and j is the index of existing capacity outage state, C_j, such that $C_j = X - C$. F_i and F_j are cumulative frequencies of states i and j respectively.

3.2.2 Load Model

The load model is usually expressed in the form of probability and frequency distribution of the random variable that represents system load [93,95]. The load model can be constructed by scanning the hourly load data of the system over the time period of study, usually one year. In general, the load model can be built in terms of load level L_i with its commutative probability and frequency as follows [93,95].

$$P_L(L \geq L_i) = \frac{H(L \geq L_i)}{T}, \tag{3.6}$$

$$F_L(L \geq L_i) = \frac{\Gamma\left(L < L_i \rightarrow L \geq L_i\right)}{T}, \tag{3.7}$$

where $H(L \geq L_i)$ is the number of hours that the hourly load is greater than or equal to the load level L_i, T is the number of hours in the interval, $P_L(L \geq L_i)$ is the commutative probability of the load level L_i, $\Gamma\left(L < L_i \rightarrow L \geq L_i\right)$ is the number of transitions from $(L < L_i)$ to $(L \geq L_i)$, and $F_L(L \geq L_i)$ is the commutative frequency of L_i.

3.2.3 Generation Reserve Model

The generation reserve margin has been used to estimate the reliability indices. The generation reserve margin model consists of the probability and frequency of a random variable M, which represents the difference between the available generation and load [93, 95]. Though the rigorous derivation of the generation reserve margin model will not be reproduced here, some expressions will be presented and explained by means of simple arguments to derive expressions for analytically determining the capacity value of VERs. The reserve margin model can be expressed in terms of generation and load model as follows [93, 95].

$$M = C_C - C_O - L, \tag{3.8}$$

where C_O is the capacity outage, L is the system load, and C_C is the net available generation capacity for commitment which can be expressed as follows.

$$C_C = C_i - C_{OP}, \tag{3.9}$$

where C_i is the installed capacity, C_{OP} is the capacity on planned outage.

For each generation reserve margin level, M_i, the cumulative probability and cumulative frequency can be calculated using (3.10) and (3.11) respectively.

$$P\left(M \leq M_i\right) = \sum_{j=1}^{n_G} \left[P_G\left(C_j\right) - P_G\left(C_j + 1\right)\right] \times P_L\left(C_C - C_j - M_i\right), \tag{3.10}$$

$$F\left(M \le M_i\right) = \sum_{j=1}^{n_G} \left[F_G\left(C_j\right) - F_G\left(C_j + 1\right)\right] P_L\left(m_{ij}\right)$$
$$+ [P_G(C_j) - P_G(C_j + 1)] F_L(m_{ij}). \quad (3.11)$$

where n_G is the number of states in the generation model (the COPAFT), C_j is the capacity outage level, $m_{ij} = C_C - C_j - M_i$, and $P_G(\bullet)$ and $F_G(\bullet)$ are the cumulative probability and frequency of the generation model respectively.

3.2.4 Calculation of Reliability Indices

The indices that have been most commonly used in power system reliability analysis are defined as follows:

A. *Loss of Load Probability* (LOLP):

A *Loss of Load* (LOL) event is one in which a system is unable to meet its total demand. The LOLP index is the probability of encountering one or more LOL events during a given time period. In general, the LOLP is given by (3.12) [93].

$$LOLP = \sum_{i=1}^{n} P(LOL_i), \quad (3.12)$$

where LOL_i is the ith LOL event, $P(LOL_i)$ is its probability, and n is the total number of LOL events encountered during the time period of study.

For the purpose of illustration, consider the CDF of a typical generation reserve margin as shown in Figure 3.5. The LOLP index can be calculated from the generation reserve margin, which is the probability of the smallest margin level as indicated in Figure

3.5 [93]. Mathematically it can be calculated as follows.

$$LOLP = P(-\Delta M), \tag{3.13}$$

where ΔM is the increment at which the probabilities of the margin are computed.

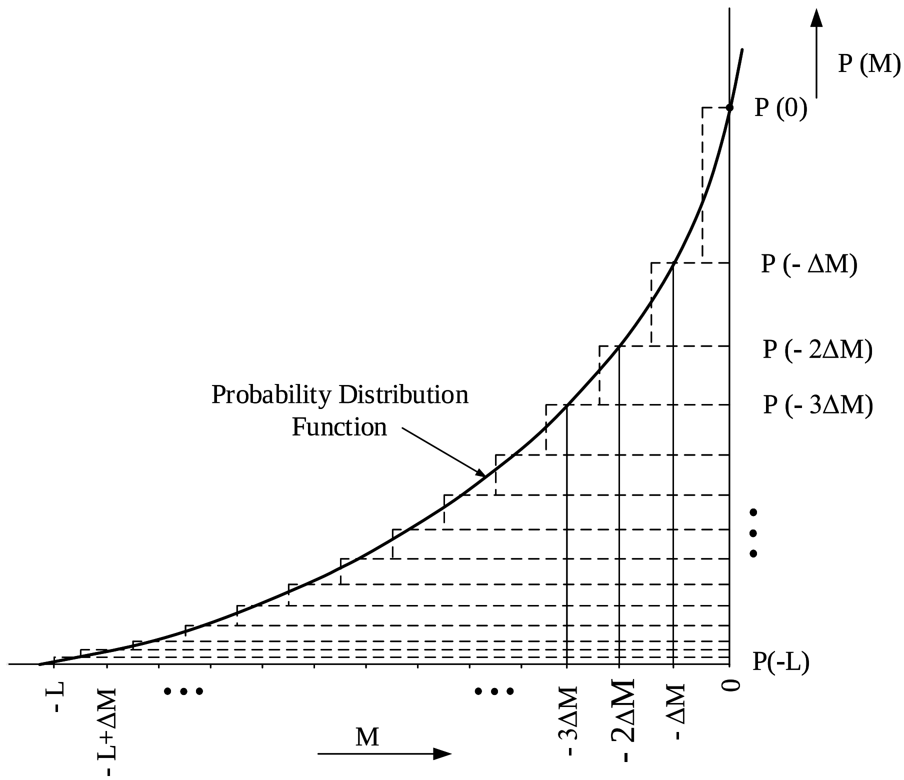

Figure 3.5 A typical cumulative probability distribution function of generation reserve margin

B. *Expected Power Not Supplied* (EPNS):

The EPNS index is the expected (average) demand that the system is unable to serve as a result of LOL events during a given time period. It is calculated as the weighted sum of the demands curtailed during the LOL events, the weights being the probabilities of the corresponding LOL events. It is expressed in MW/year or GW/year. The EPNS index is equal to the area under the probability distribution curve over the domain of $M \leq 0$ as shown in Figure 3.5 [93]. This area can be approximated by the sum of the areas of the rectangles shown in 3.5, which is given by (3.14) [93].

$$EPNS = (\Delta M)[\sum_{M=0}^{-L} P(M) - \frac{1}{2}(P(0) + P(-L))], \tag{3.14}$$

where $-L$ is the smallest (largest in magnitude) negative margin considered.

C. *Loss of Load Expectation* (LOLE):

The LOLE index is the expected number of LOL hours during a given time period. It is expressed in hr/year. LOLE index can be directly calculated by multiplying the LOLP index by the number of hours in a year as expressed in (3.15) [93].

$$LOLE = LOLP \times 8760. \tag{3.15}$$

D. *Loss of Load Frequency* (LOLF):

The LOLF index is the expected frequency of encountering one or more LOL events during a given time period. The LOLF index can be calculated using (3.16) [93].

$$LOLF = F(-\Delta M). \tag{3.16}$$

E. *Loss of Load Duration* (LOLD):

LOLD index identifying the average deficiency of encountering one or more LOL events during a given time period.The LOLD index can be calculated using (3.17) [93].

$$LOLD = \frac{LOLP}{LOLF}. \tag{3.17}$$

These reliability indices are used to assess the reliability performance of a generation system. In the evaluation process, the generation model is convoluted with generation model to obtain system indices. The process of convolving the generation model and load model is explained in [94].

3.2.5 Simulation Methods

Mote Carlo simulation able to capture a wide range of modeling detail and system dependencies,especially when systems are too complex to solve with analytical methods. The operation characteristics of VERs, such as correlation, input fluctuation, and the random failure of generating units, can be mimicked by sequential simulation. Monte Carlo simulation is a flexible technique, applicable to simulate the operation behavior of complex systems, and can easily be implemented to determine reliability indices. On the other hand, Monte Carlo simulation becomes time consuming, especially when implemented in a large and complex system. Further, the solution accuracy depends mainly on the number of sampling performed to produce the output [96, 97]. However, the purpose of this research is to construct a model for a cluster of VERs, and Monte Carlo simulation is normally not considered appropriate for model building. A direct, analytical method is considered a better approach for building reliability models. In this work, therefore, Monte Carlo is used only for model validation.

Chapter 4

Comprehensive Models of Variable Resources

4.1 Introduction

In this work an analytical method is described for constructing a reliability model of a wind farm and a PV system, an analytical method is used to construct a generation model for both wind farms and PV system. The generation model that represents the output power of VERs is denoted in this work in terms of COPAFT. A COPAFT represents a combination of capacity levels with the probabilities of existence and cumulative probabilities to represent the probability distribution function of the outage states.

4.2 Wind Power

In this work an analytical method is described for constructing a reliability model of a wind farm, considering turbine correlation, output variability, and forced outages. The resulting model resembles a multi-state generating unit with probability and frequency distributions of the discrete capacity states, expressed in the form of a capacity outage probability and frequency table (COPAFT) [98,99]. This affords the advantage that now the entire wind farm can be treated as a single, equivalent generating unit that can be incorporated in traditional probabilistic planning methods, without further regard to the correlation between turbines within the farm. In constructing the proposed wind farm model, several distinctive and innovative approaches are utilized. These contributions are summarized below and described further in section 4.3.

1. The number of states is reduced without compromising the model accuracy. This is achieved by first converting the time series wind speed data into turbine output power and then clustering the output power data, which is less dispersed and easier to cluster. The method considers transition of output power between all clusters, not just adjacent clusters (unlike a birth-death process).

2. The model is comprehensive in that it captures (a) wind variability, (b) turbine outages, and (c) WTG output correlations. This is achieved by separately modeling the independent outages of wind turbines and the dependency on wind speed, and then convolving the two distributions. The overall approach is depicted in Figure 4.1.

3. A generalized approach is developed for calculating not only the probabilities but also the frequencies within the multi-state convolution process described above, where the tracking of transitions between so many states is fairly complex.

4.2.1 Attributes of Wind Power Output

In power system reliability assessment, several wind power models have been utilized to calculate the output power of wind farms. For instance, the actual value and the mean value of the recorded wind speed data at certain wind farm locations have been utilized to estimate the outputs of WTGs [100, 101]. The output of wind turbines are known to vary with wind speed and the design characteristics of wind generators. This section describes the characteristics of wind power in terms of WTG output power and the correlation between the output of WTGs and changes in the wind speed across the farm.

4.2.1.1 Wind Turbine Output Power Curve

Wind turbine power curve provides a quantitative relationship between wind speed and the output power. It describes the operational characteristics of a WTG. The output power that can be extracted from wind turbines can be calculated as follows [102].

$$P = \frac{1}{2} C_p \rho A v^3, \tag{4.1}$$

where P is the output power (watts), ρ is the air density (kg/m^3), v is the wind speed (m/sec), A is the swept area of the turbine (m^2), and C_p is the power coefficient.

The output power curve combines (4.1) with the physical constrains in the system. The output power curve including the physical constraints can be expressed as follows.

$$P = \begin{cases} 0, & \text{if } v < v_{cut\text{-}in} \\ \frac{1}{2}\rho A C_p v^3, & \text{if} v_{cut\text{-}in} \leq v < v_r \\ P_r, & \text{if } v_r \leq v < v_{cut\text{-}out} \\ 0, & \text{if } v_{cut\text{-}out} \leq v \end{cases}, \tag{4.2}$$

where $v_{cut\text{-}in}$ is the designed cut-in speed, $v_{cut\text{-}out}$ is the designed cut-out speed, v_r is the rated speed and P_r is the rated power of the wind turbine.

4.2.1.2 Correlation Between Turbine Outputs

In the literature on power system reliability modeling, several studies have investigated the effect of the correlation between the output power of WTGs and the change in the wind speed within the same farm [103–109]. The degree of the correlation depends on several factors such as geographic location, separation distances between WTGs, terrain and number of WTGs on the wind farm and the influence of the resulting to wake effect and turbulence [110–112]. These correlations also vary with time scales (the frequency of wind speed observations can be intervals of 5 minutes, 10 minutes, hourly, etc.). Thus, determining the exact degree of correlation between individual WTGs and the change in the wind speed within the same farm is a challenging and complex task particularly for large wind farms [113]. However, it has been reported that WTGs within a wind farm are approximately driven by same values of wind speed and the power outputs of WTGs show consistent behavior among individual WTGs with the change in the wind speed on the entire farm [105–109]. Despite individual variation of WTGs output, it can be safely assumed that there is an average behavior among wind turbines without excessive deviation across the farm. This simultaneously captures the correlation across the farm.

4.2.1.3 Correlation with Other Stochastic Elements

Correlations have also been observed between wind production and other stochastic elements that are considered in power system analyses. For instance, [114] reports negative correlations between wind and solar production, and [115] reports positive, negative, and negligible correlations between wind production and system loads depending on time scales, time of day, and seasons. While some researchers [14, 50] have modeled the correlation with load, others [116] have postulated that the correlation is negligible. Moreover, the impact of correlation is also affected by such factors as differences in scale (sizes of wind or solar installations and load), geographic location, and electrical distances between points of insertion. Another challenge in modeling correlation between wind production and system load is that most of these models treat wind injections as negative loads, inherently assuming that all energy that can be produced by a wind farm is completely accepted by the system. Despite wind production being designated as "must take" in many regulatory regimes, it is well known that prevailing system conditions such as low loads or network congestion often necessitates spillage of wind generation. In view of the above reasons, as well as the fact that the stated intent of the work reported here focuses on the construction of a reliability model of the production of a wind farm, this work does not attempt to model correlations between wind production and other stochastic elements. It does, however, evaluate some of the impacts in the case studies.

4.3 Reliability Modeling of Wind Farms

In this work an analytical method is described for constructing a reliability model of a wind farm, considering turbine correlation, output variability, and forced outages. The resulting model resembles a multi-state generating unit with probability and frequency distributions of the discrete capacity states, expressed in the form of a capacity outage probability and frequency table (COPAFT) [117]. This affords the advantage that now the entire wind farm can be treated as a single, equivalent generating unit that can be incorporated in traditional probabilistic planning methods, without further regard to the correlation between turbines within the farm. In constructing the proposed wind farm model, several distinctive and innovative approaches are utilized. These contributions are summarized below and described further

- The number of states is reduced without compromising the model accuracy. This is achieved by first converting the time series wind speed data into turbine output power and then clustering the output power data, which is less dispersed and easier to cluster. The method considers transition of output power between all clusters, not just adjacent clusters (unlike a birth-death process).

- The model is comprehensive in that it captures (a) wind variability, (b) turbine outages, and (c) WTG output correlations. This is achieved by separately modeling the independent outages of wind turbines and the dependency on wind speed, and then convolving the two distributions. The overall approach is depicted in Figure 4.1.

- A generalized approach is developed for calculating not only the probabilities but also the frequencies within the multi-state convolution process described above, where the tracking of transitions between so many states is fairly complex.

4.3.1 Modeling of Forced Outages of WTGs

In the assessment of the effect of wind power on power system reliability, failures of WTGs have a significant impact on the available power [118–122]. Several studies show that the size of turbines, operation and environmental factors could lead to different failure modes of wind turbines. Failures of WTGs usually occur due to ageing, worn out parts or manufacturing defects [118–121]. Considering failures of WTGs as *independent* events, the probability of failure of WTG can be modeled as Markovian components with two states, *up* and *down* states with known failure and repair rates, λ and μ respectively (λ is the failure transition rate from an *up* state to a *down* state, and μ is the repair transition rate from a *down* state to an *up* state). Based on the FOR (forced outage rate is the failure probability) of turbines,

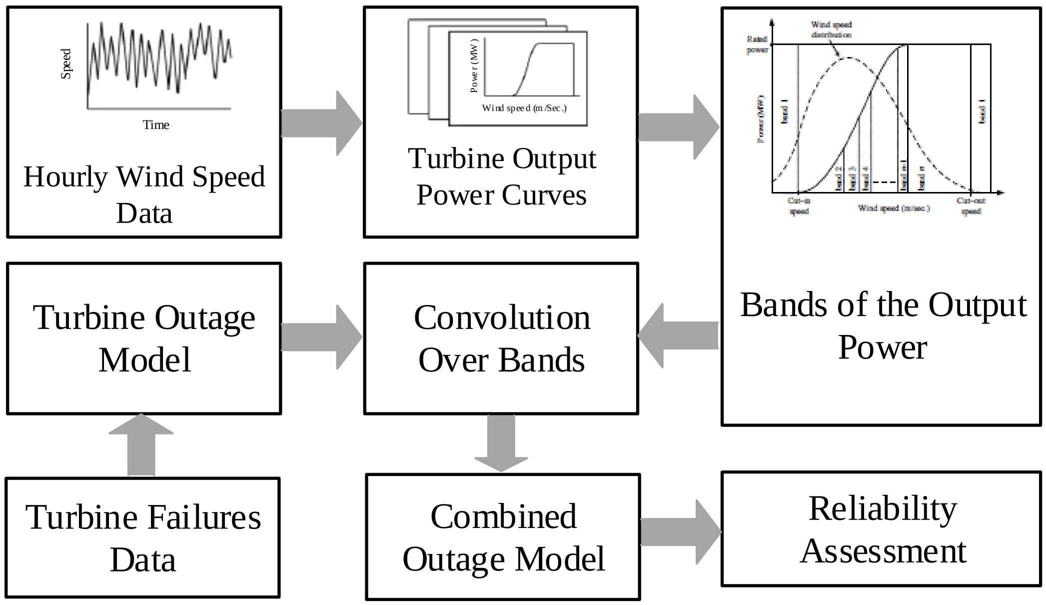

Figure 4.1 Model combining wind variability and turbine failures

the $\mathrm{COPAFT_f}$ of wind turbines can be built using the *unit addition algorithm*. This is a recursive algorithm that starts with the distribution of one unit (a WTG in this case) and successively convolves with it the distributions of the remaining units, one unit at a time. In general, when adding a new unit of capacity C, forced outage rate q and failure frequency μ, the cumulative probability and frequency of an outage state X can be determined by the following expressions [94].

$$P(X) = \bar{P}(X)(1-q) + \bar{P}(X-C)q \tag{4.3}$$

where $P(X)$ and $\bar{P}(X)$ denote the cumulative probabilities of the capacity outage state before and after the units are added.

Equation (4.3) is initialized as follows.

$$P(X) = \begin{cases} 1, & \text{if } X \leq 0 \\ \\ 0, & \text{otherwise,} \end{cases}$$

The cumulative probability $P(X)$ for a forced outage of X MW or greater can be in general represented by (4.4).

$$P(X) = \sum_{i} P(X_i), \quad \forall\ X_i \leq X, \tag{4.4}$$

where

$$\bar{P}(X) = 1, \quad \forall\ X \leq C$$

In the case of multi-state generating units, (4.3) can be modified as follows.

$$P(X) = \sum_{i=1}^{n} P_i \times \bar{P}(X - C_i). \tag{4.5}$$

The cumulative frequency $F(X)$ of capacity outage X can also be calculated using the same approach, as shown in (4.6).

$$F(X) = F_i\,(1 - q) + F_j q + (P_j - P_i) q\mu, \tag{4.6}$$

where P_i, P_j, F_i, and F_j are determined from the old COPAFT; i is the index of the existing capacity outage state $C_i = X$ and j is the index of existing capacity outage state C_j such that $C_j = X - C$; F_i and F_j are cumulative frequencies of states i and j respectively.

4.3.2 Clustering of WTG Outputs

The first step in the proposed method consists of converting the wind speed time-series data into output power data using (4.2). The values of wind power that correspond to the observed wind data are clustered into several bands (states) based on their similarities. In the clustered wind power, every observation belongs to one and only one band based on minimum Euclidean distances between the observed data points. By converting the observed wind speed into power using power curve characteristics of WTGs, several dissimilar and often different observed wind speed points (that result in similar output powers) will be grouped in the same bands. For example, wind speeds that range from 0 (m/sec) to the cut-in speed of the WTG and the wind speeds range from the cut-out speed of WTG to the maximum observed value are grouped in one band, i.e., the band that have zero output power which is denoted band 1 in Figure 4.2. Also, wind speeds that range from the rated speed of WTG to the cut-out speed of WTG are grouped in one band (band n in Figure 4.2).

4.3.3 Combining Variability and Failure Models

A capacity outage probability and frequency table for a wind farm can be constructed by combining the $\mathrm{COPAFT_f}$ that represents the rated capacities and failures of WTGs (section 4.3.1) and the clustered wind power table (section 4.3.2). The $\mathrm{COPAFT_f}$ is convolved over each wind power band to construct a COPAFT for the entire wind farm ($\mathrm{COPAFT_c}$).

This section explains the combination procedure of these two tables. Figure 4.3 shows the process of combining the outages of wind power due to (1) wind power transitions between bands and (2) failures of WTGs. Horizontal transitions represent the transitions due to the

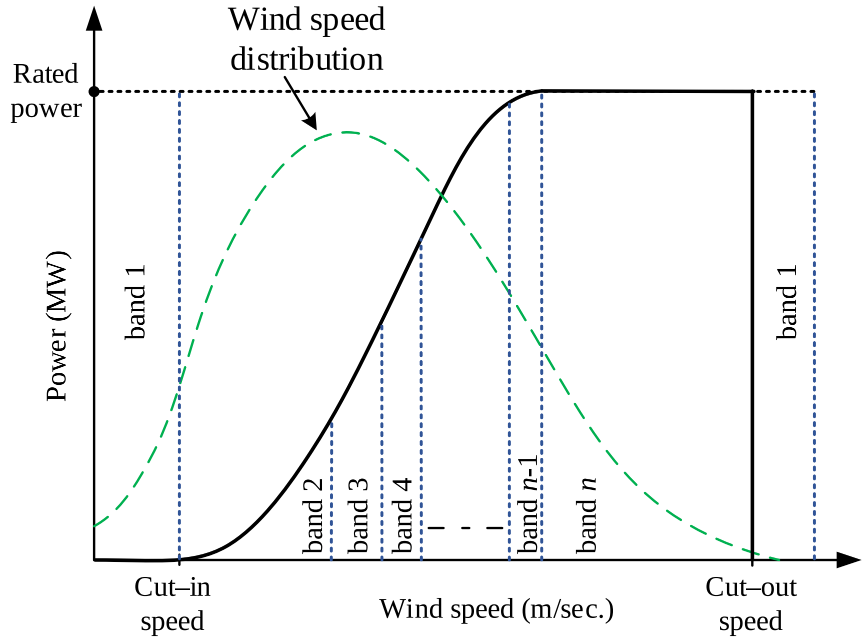

Figure 4.2 Bands of the output power and wind speed distribution

change in the wind power between bands and vertical transitions represent transitions due to failures of WTGs. The new outage states due to wind power band transition and failures can be obtained by scanning through all bands in both vertical and horizontal directions. In convolving the states of the ($\mathrm{COPAFT_f}$) of wind turbines over each band, the capacity outage state i in the ($\mathrm{COPAFT_c}$) with $C_o \geq X$ occurs in both vertical and horizontal directions.

The procedure of the proposed method of clustering wind power into bands, modeling failures of WTGs and building the generation model ($\mathrm{COPAFT_c}$) for a wind farm is summarized in the following steps:

1. From the observed wind speed data and the output power curve of WTGs, determine the output power time series of the wind farm.

2. Use nearest centroid sorting to cluster the output power into bands; then calculate the cluster (band) means, cluster probabilities, and inter-cluster transition rates.

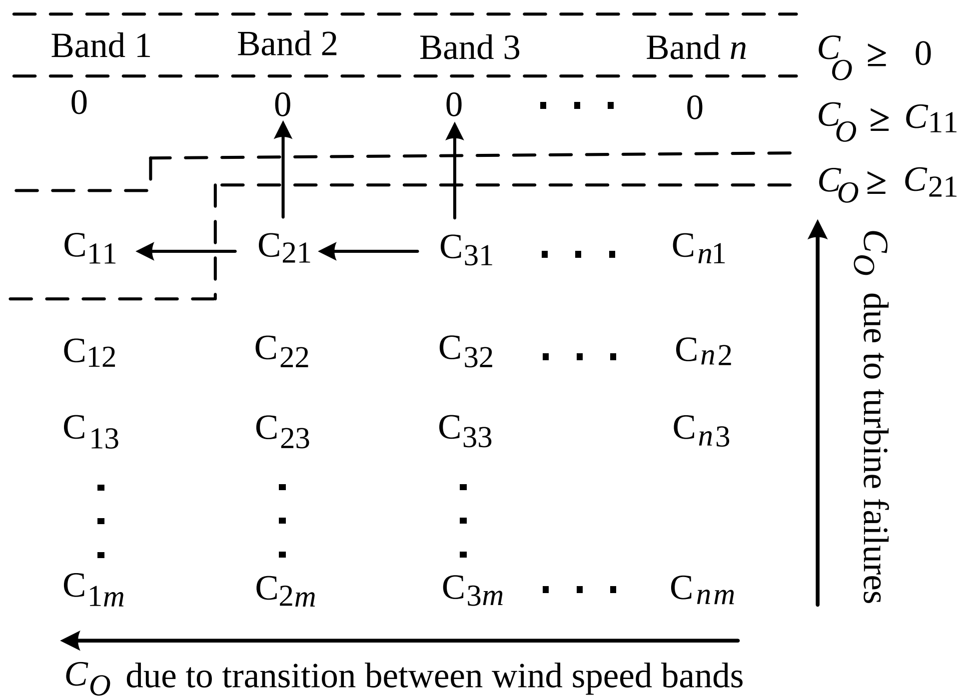

Figure 4.3 The combined outage due to transition of wind power (horizontal transitions) and failures of wind turbines (vertical transitions)

3. Build the COPAFT_f of WTG using the method presented in section 4.3.1.

4. Convolve the COPAFT_f with the probability and frequency of each wind power band. The failure and repair rates of the WTGs remain the same in each band. Only the output power changes from band to band due to the effect of wind power transition from stat from state k to state $k+1$.

5. The available capacity and capacity outage for state i in COPAFT_f that exists in band k can be calculated using (4.7) and (4.8) respectively.

$$M_{i,k} = \frac{A_i}{C_R} \times W_k, \tag{4.7}$$

$$O_{i,k} = C_R - M_{i,k}, \tag{4.8}$$

where $M_{i,k}$ is the new available capacity in state i of the COPAFT$_\text{f}$ being in band k, A_i is the available capacity in state i of the COPAFT, C_R is the total installed capacity of wind farms, W_k is the available wind power in band k and $O_{i,k}$ is the new outage capacity of state i of the COPAFT$_\text{f}$ being in band k.

6. The probability of the new outage state is given by

$$P_{i,k} = \sum P_{W(k)} \times P_{M(i)}, \tag{4.9}$$

where $P_{i,k}$ is the probability of outage capacity of state i being in band k, $P_{W(k)}$ is the band probability, and $P_{M(i)}$ is the COPAFT$_\text{f}$ state outage probability.

7. The cumulative outage probability of an outage state with $C_o \geq X$ can be obtained by scanning through all bands. Whenever an outage state with outage capacity of $C_o \geq X$ is encountered, its probability is accumulated as follows.

$$P\left(C_o \geq X\right) = \sum_{i=1}^{n} \sum_{k=1}^{m} P_{i,k}, \tag{4.10}$$

where n is the number of COPAFT$_\text{f}$ states and m is the number of bands.

8. Scan through all states in the COPAFT$_\text{c}$ and combine the duplicated states.

9. The transition rates of wind power between bands from state i in band (k) to state $(i+1)$ in band $(k+1)$ is given by (4.11). The exact transition rates between bands are considered [14].

$$\lambda = \frac{n_{(i \to i+1)}}{D}, \tag{4.11}$$

where $n_{(i \to i+1)}$ counts the number of wind power transitions between bands from state

$(wp_i < wp)$ to $(wp \geq wp_i)$ and D is the time period of study.

10. The frequency of wind power of band (k) can be calculated by

$$f_{W(k)} = P_{W(k)} \times \lambda, \tag{4.12}$$

11. The cumulative outage frequencies of encountering an outage state with an outage capacity of $(C_o \geq X)$ due to the transition of COPAFT_f states between wind power bands can be calculated by (4.13).

$$F\left(C_o \geq X\right) = F_k + F_{WTG}, \tag{4.13}$$

where

$$F_{WTG} = \sum P_{W(k)} \times F_{M(i)} \tag{4.14}$$

where $F_{M(i)}$ is the cumulative outage frequency of i^{th} outage state and,

$$F_k = \sum P_{M(i)} \times f_{W(k)}. \tag{4.15}$$

As a result, the reliability model of wind farms can be represented by single generation unit with multiple states.

4.4 Model Validation and Test Results

The resulting COPAFT_C of a wind farm can now be treated as the reliability model of a single equivalent unit with multiple states [94], for purposes of generation adequacy analysis or composite reliability analysis. In this work, we have evaluated the most common indices that have been used in power system reliability analysis to test the proposed method. In this work, we have evaluated the most common indices that have been used in power system reliability analysis to test the proposed method. These indices are LOLP, EDNS, LOEE, LOLE and LOLF.

4.4.1 Test System

The proposed method is applied on the IEEE RTS [123]. This system has been extensively used in the literature for purposes of benchmarking. The IEEE RTS consists of 32 generating units with total generation capacity of 3405 MW and total peak load of 2850 MW. The single line diagram of this test system is shown in Figure 4.4.

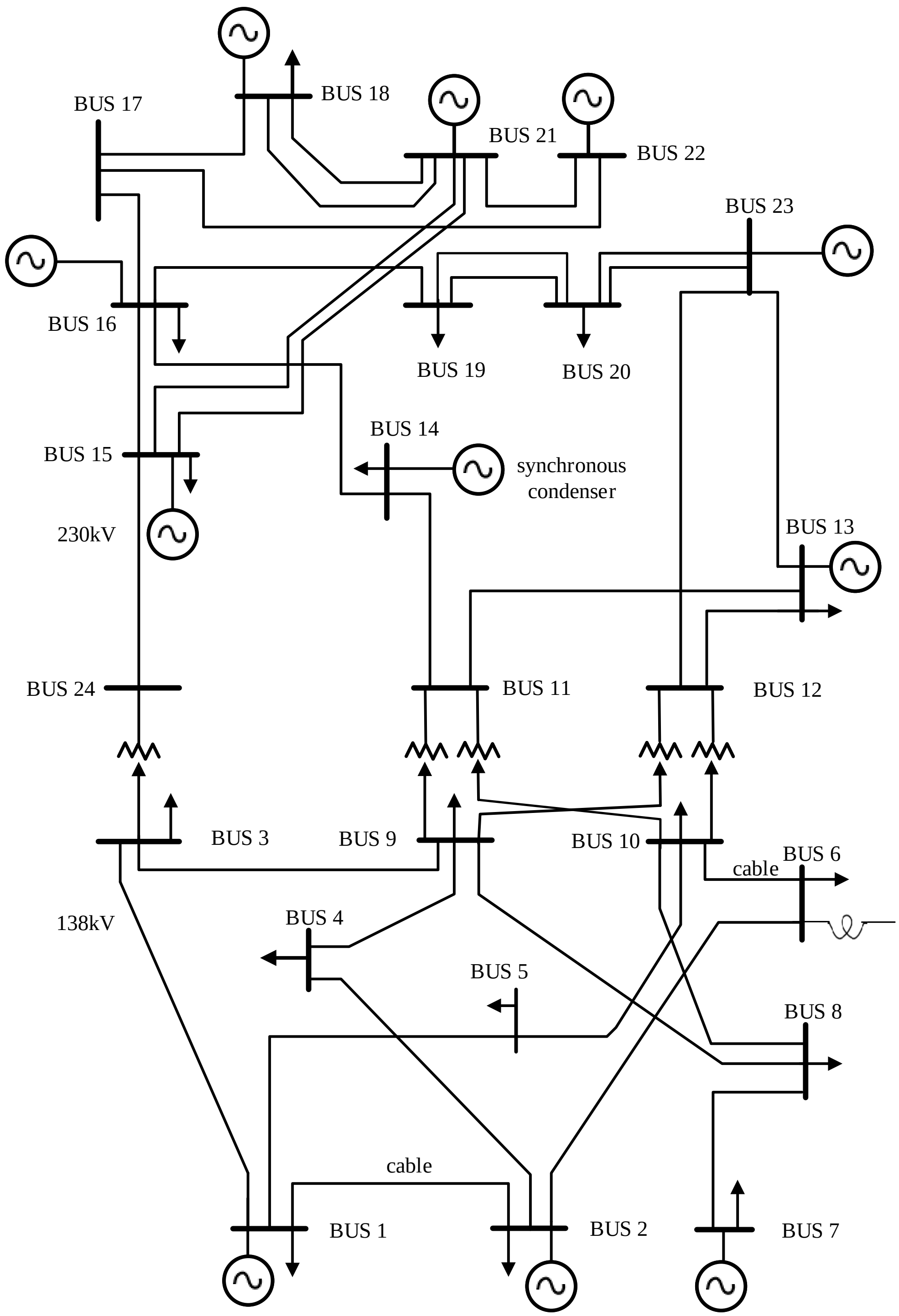

Figure 4.4 Single line diagram for IEEE-RTS

4.4.2 Case Studies

In this case studies, a typical wind turbine characteristic is assumed (type Vesta V90-3.0 MW [124]); rated power: 3 MW; rated, cut-in and cut-out speeds: (15 m/sec., 3.5 m/sec., 25 m/sec.). In the cases reported here, the effect of different values of WTG failure probabilities were studied, and the reliability data used are shown in Table 4.1. The failure rates and mean time to failure (MTTF) shown here lie in the ranges for actual WTGs, as reported in [125]. Repair times are calculated from the FORs and failure rates of WTGs and are expressed as mean time to repair (MTTR)

Table 4.1 Wind Turbine Reliability Data Used in the Test Cases

FORs	λ (failure/yr)	MTTF (hour)	MTTR (hour)
0.04	2.43333	3600	150
0.08	2.72050	3220	280
0.12	3.61983	2420	330

Three wind data sets are used: data set A [126], data set B [127], and data set C [128]. The correlation coefficients between these data sets and the load of the IEEE RTS are as follows: (1) -0.002 for data set A, (2) 0.0686 for data set B, and (3) -0.1059 for data set C. Whereas data set A and the load are almost uncorrelated, data set B has positive correlation and data set C has negative correlation with the load. A wind farm consisting of 50 WTGs (150 MW total capacity) is added to the IEEE RTS. In the case studies reported below, this farm is assumed to be subjected to each of the three wind speed data sets. For convenience, these are referred to as *Farm A*, *Farm B*, and *Farm C*. In each case, the outputs of the corresponding wind farm are grouped into ten clusters. As an illustration, Table 4.2 shows the mean output of each band, individual and cumulative probabilities, and the cumulative frequencies of transition across bands of wind output for the *Farm A*. The $\mathrm{COPAFT_f}$ of WTGs is built using the reliability data corresponding to FOR of 0.04 shown in Table 4.1, and then convolved with the distributions of the farm output power bands (variability model) using the procedure described in section 4.3.1 to produce the combined COPAFT, i.e., COPAFT_C. Table 4.3 is the COPAFT_C of Farm A. The COPAFT_C shows the available capacity C_i, individual and cumulative probabilities, and the cumulative frequency of each wind output state i.

Table 4.2 Reliability Model: Farm Output Bands and Probabilities

No.	Output Power (MW)	Exact State Probability	Cumulative Probability	Cumulative Frequency
1	0	0.13653	1	0
2	8.59	0.17648	0.86347	0.1862
3	20.55	0.13025	0.68698	0.3892
4	40.58	0.14486	0.55673	0.4226
5	58.04	0.08482	0.41187	0.2978
6	74.64	0.03721	0.32705	0.3158
7	94.37	0.05993	0.28984	0.2836
8	117.15	0.02819	0.22991	0.2396
9	125.55	0.03025	0.20171	0.1860
10	149.23	0.17146	0.17146	0.1301

Generation adequacy or composite system reliability assessment can be performed by using a multi-state model such as that shown in Table 4.3 to represent the output of the wind farm. In the next section, the following case studies are presented: (1) reliability analysis including forced outages of WTGs, (2) the effect of correlation between wind power and system load on reliability indices, and (3) determination of capacity values of wind farms.

4.4.2.1 Reliability Analysis–Base Case

In this section, the reliability indices of the IEEE RTS are calculated prior to adding the wind farm. These indices are calculated using discrete convolution and Monte Carlo simulation. The results are shown in Table 4.4 where the second row shows the reliability indices of the

Table 4.3 Reliability Model: Farm Output States and Probabilities

No. i	Output Power (MW) C_i	Exact State Probability $P\{C = C_i\}$	Cumulative Probability $P\{C \geq C_i\}$	Cumulative Frequency $F\{C \geq C_i\}$
1	0	0.003133	1	0
2	2.984	0.013057	0.9968662	0.0037882
3	5.968	0.026658	0.9838091	0.0080676
4	8.953	0.035544	0.9571506	0.0112011
5	11.937	0.034804	0.9216061	0.0114028
6	14.922	0.026683	0.8868021	0.0090757
7	17.906	0.016676	0.8601190	0.0058807
8	20.891	0.008735	0.8434421	0.0031896
9	23.875	0.014417	0.8347065	0.0035518
10	29.844	0.013514	0.8202890	0.0085116
11	34.415	0.013085	0.8067750	0.0207453
12	39.101	0.033351	0.7936900	0.0349233
13	43.787	0.017900	0.7603390	0.0286773
14	47.751	0.008530	0.7424390	0.0074431
15	71.903	0.023100	0.7339090	0.1055822
16	90.714	0.037809	0.7108090	0.0648995
17	99.316	0.081800	0.6730000	0.1159003
18	129.085	0.160200	0.5912000	0.2455493
19	140.974	0.162100	0.4310000	0.1444312
20	149.223	0.268900	0.2689000	0.1188310

IEEE RTS as calculated using Monte Carlo simulation.

Table 4.4 Reliability Indices of the IEEE RTS (Base Case)

Method	LOLP	LOLE hr/yr	LOLF occ./yr	LOLD yr	EDNS MW/yr	LOEE MWh/yr
DC	0.001069	9.36881	2.01600	4.64723	0.1348396	1181.195
MCS	0.001070	9.37407	2.01800	4.64522	0.1349867	1182.483

DC: Discrete convolution; MCS: Monte Carlo simulation

4.4.2.2 Reliability Analysis–After Adding Wind Farm A

In this case study, the IEEE RTS with Farm A added is used to test the proposed method and to investigate the effect of forced outages of WTGs on the reliability indices. The rated capacity of the wind farm is 150 MW. The reliability indices are evaluated for different values of FOR as shown in Table 4.5. As expected, ignoring the WTG failures in adequacy studies produces optimistic results.

Table 4.5 Annual Reliability Indices of the IEEE RTS After Adding Farm A Considering Different Values of Turbine FOR

Method	LOLP	LOLE hr/yr	LOLF occ./yr	LOLD yr	EDNS MW/yr	LOEE MWh/yr
0.04	0.0007664	6.713700	1.603389	4.187400	0.093696	820.778
0.08	0.0007756	6.794491	1.626876	4.176403	0.094894	831.270
0.12	0.0007852	6.878366	1.645477	4.180165	0.096148	842.254

4.4.2.3 Reliability Analysis–After Adding Wind Farm A Using Monte Carlo Simulation

In this case study, Monte Carlo simulation is also performed on the same system (with *Farm A*), and the results are very close to those calculated using the proposed method as shown in Table 4.6. This observation is not surprising since the wind speeds for Farm A are almost uncorrelated with the load.

Table 4.6 Annual Reliability Indices of the IEEE RTS After Adding Farm A Considering Different Values of Turbine FOR, Using Monte Carlo Simulation

Method	LOLP	LOLE hr/yr	LOLF occ./yr	LOLD yr	EDNS MW/yr	LOEE MWh/yr
0.04	0.0007642	6.694428	1.603279	4.175438	0.093653	820.401
0.08	0.0007748	6.786822	1.619107	4.173034	0.094841	830.808
0.12	0.0007876	6.899390	1.647222	4.188492	0.096248	843.130

4.4.2.4 Effect of Correlation with Load

To investigate the effect of correlation between wind speed and load, the results of adding Farms B and C to the IEEE RTS are studied. The reliability indices, as calculated analytically by convolving the multi-state farm model with the generation model of the IEEE RTS are compared with those obtained from Monte Carlo simulation. (For simplicity, turbine failures are neglected, as they have no effect on correlation with load.) Since the Monte Carlo method uses a sequential simulation that tracks hourly load and wind production, thereby intrinsically capturing their correlation, it enables us to assess the error introduced by ignoring the correlation in the proposed analytical method. Table 4.7 shows the reliability indices after adding Farm B to the IEEE RTS. The results in Table 4.7 show that for Farm B, where there is a positive correlation between wind speed and load, the proposed method produces pessimistic results with an average error of -2.17%.

Table 4.7 Reliability Indices of the IEEE RTS After Adding Farm B

Method	LOLP	LOLE hr/yr	LOLF occ./yr	EDNS MW/yr	LOEE MWh/yr
Proposed	0.00067	5.90528	1.41762	0.080620	706.248
MCS	0.00065	5.69402	1.33438	0.080138	702.011

Table 4.8 shows the reliability indices after adding Farm C to the IEEE RTS. These results show that for Farm C, where there is a negative correlation between wind speed and load, the proposed method produces optimistic results with an average error of 2.07%.

Table 4.8 Reliability Indices of the IEEE RTS After Adding Farm C

Method	LOLP	LOLE hr/yr	LOLF occ./yr	EDNS MW/yr	LOEE MWh/yr
Proposed	0.0007998	7.005971	1.558705	0.0974247	853.4403
MCS	0.0008132	7.124022	1.598659	0.0994838	871.4785

The above results show that the proposed method is effective in building an accurate reliability model of a wind farm, but small errors are introduced in adequacy analyses due to external correlations. However, where the benefits of being able to use an equivalent model in analytical studies outweigh those of detailed Monte Carlo simulation, as well as for the reasons discussed in section 4.2.1.3, the proposed method offers the advantage of producing an accurate and reusable model.

4.5 Photovoltaic (PV) Systems

Different topologies of PV systems have been addressed in literature [129, 130, 130]. In general, topologies of PV systems are mainly classified based on the arrangement of PV panels and DC/DC and DC/AC converters. These arrangements are usually set up to enhance the system efficiency and reliability. Grid-connected PV systems are usually constructed from a large number of components such as power electronic circuits and solar panels. The reliability of such components is highly dependent upon the operation and ambient conditions. Operational and environmental factors may lead to overall reduction in the output power and failure of system components [30, 131, 132]. Modeling of these systems in power system reliability is a complex task due to the dependency of the output power on the intermittent source (solar radiation) and the availability of a large number of system components. An analytical method to construct a capacity outage probability and frequency table (COPAFT) that captures both the intermittency of the input source and component failures can be built using the same approach used for wind power as explained in section 4.3.

4.5.1 Attributes of PV System

In PV systems, power electronic systems are considered major components. These component play an important role and high efficient solutions to power conversion. However, the large number of power electronic devices and the failure of power electronic circuits leads to more challenges into the evaluation process of the reliability of the overall systems. One of the concerns related to reliability lies in the power semiconductor devices and electrolytic capacitors that are the most vulnerable links. Most of power electronic converters are not equipped with redundancy. Therefore, any fault that occurs to the components or subsystems of the system will lead to shutdown of the system. From reliability point of view, such components should be considered in evaluating the adequacy of PV systems. Due to large number of system components of PV systems, only the reliability of major components have been considered [30,131,132]. For power system adequacy, when PV power is introduced to the main grid, its necessary to investigate the effect of all system components.

4.5.2 Grid Level PV Farm Structure

In general, a PV farm is constructed from a large number of PV panels arranged in arrays. The PV arrays are constructed from PV panels which in turn are connected to the main grid through DC/AC inverters. A set of N panels in each array is called sub-array. PV panels are constructed from a large number of solar cells in series configurations. At the higher level, the output of the PV system is then connected to the grid through a power transformer [13], [15]. The amount of the output power of a PV farm at a certain location depends on the input availability (mainly solar radiation) and the availability of system components. In a PV farm, since PV panels are placed adjacent to each other, all PV panels are assumed to have the same solar radiation, and approximately experience the same operational and environmental factors that may affect the output of the farm.

4.5.3 Output Power of PV Systems

The maximum output power ratings of PV systems are provided by the manufacturer and usually are expressed in peak-watt (W_P). The currentvoltage characteristics ($I - V$ characteristics) under the standard test conditions (the radiation level of 1 kW/m^2 is given for temperature of 25° C) can be calculated using the following relationships [133]:

$$I = s\left[I_{sc} + K_I(T_c - 25)\right], \tag{4.16}$$

$$V = V_{oc} - K_V T_c, \tag{4.17}$$

where s is the radiation level, I_{sc} is the short circuit current, K_I is the short circuit current temperature coefficient in $A/°C$, V_{oc} is the open circuit voltage, K_V is the open circuit voltage temperature coefficient in $V/°C$ and T_c is the cell temperature in $°C$ which can be expressed as follows [133]:

$$T_c = T_a + s\left(\frac{T_{no} - 20}{0.8}\right), \tag{4.18}$$

where T_a is the ambient temperature and (T_{no}) is the nominal operating temperature of the cell ($°C$).

The output power (P_{pv}) for a given radiation level, ambient temperature and the current-voltage characteristics can be calculated using the following relationships [133]:

$$P_{pv} = N \times FF \times I \times V, \tag{4.19}$$

where N is the number of panels and FF is the fill factor, which depends on the module characteristics, and can be expressed as follows [133]:

$$FF = \frac{V_{mpp} I_{mpp}}{V_{oc} I_{sc}}, \tag{4.20}$$

where V_{mpp} and I_{mpp} are the current and voltage at the maximum power point.

4.5.4 Attributes of PV System Components

In a PV farm, power electronic devices play an important role. Power electronic circuits deliver the output power of PV panels to the load or to the grid. Reliability assessment of power electronic circuits of large-scale grid-connected PV systems for different topologies have been addressed in [129, 132, 134]. The major components that contribute to system failure are power electronic circuits. In the literature, the mean time to failure (MTTF) has been used as an indicator for system unavailability; the overall reliability of the circuit is calculated by summing the failure rates (the failure rate is reciprocal of the MTTF) of the components [4, 5, 135]. However, this is true if a failure of a component leads to overall failure of the power electronic circuit. In some cases such as multilevel inverters, redundancy exists in power electronic topologies and their desired function is not totally affected by a component failure [136]. In this case, there are several possible different paths that can still produce an acceptable output voltage level. In such configurations, the overall failure cannot be assumed by summing the failure rates of the components. Analytical techniques can be used to estimate system reliability such as reliability network analysis, minimal cut set, minimal path set and state enumeration techniques [137]. In general, the reliability function, $R(t)$, indicates the probability that the system will operate without failures over a time interval [0, t]. The failure rate of system component during the useful lifetime is usually considered independent of time. The reliability of system components can be expressed as an exponential function of their constant failure rate during the useful lifetime as follows.

$$R(t) = e^{-\lambda_i t}, \tag{4.21}$$

where λ_i is the constant failure rate of a power electronic component.

The mean time to repair (MTTR) has been considered small enough and can be neglected [138]. This could be a valid assumption for a small system or a system with a few components where the time required to repair or replace a component is small comparing to MTTF. However, for large systems, neglecting the repair time could produce optimistic results. Therefore, the MTTR should be included in modeling the output of PV systems. System availability and unavailability as functions of MTTF and MTTR are described by (4.22) and (4.23).

$$p = \frac{\mu}{\lambda + \mu}, \tag{4.22}$$

$$q = 1 - p = \frac{\lambda}{\lambda + \mu}, \tag{4.23}$$

where p is the probability of component availability, q is the probability of component failure and μ is the repair rate (reciprocal of $MTTR$).

For a system with N components connected in series, system availability (p^s_{sys}) can be calculated by (4.24).

$$p^s_{sys} = \prod_{i=1}^{N} p_i, \tag{4.24}$$

where p_i is the probability of availability of component i.

For parallel configuration, there might be a tolerance for the desired output, and the reliability of the system is the probability of all possible successful paths that can provide the desired output. system availability (p^s_{sys}) can be calculated by (4.25).

$$p^p_{sys} = 1 - \left[\prod_{i=1}^{N} (1 - p_i)\right], \tag{4.25}$$

In the cases of series-parallel reliability configuration, it is useful to use network reduction techniques (NRT). The availability and unavailability can then be calculated by combining all series and parallel configurations to a equivalent unit using (4.24) and (4.25).

4.5.5 Reliability Modeling of Major Components of PV Systems

In the PV systems, the major components that contribute to system failure are power electronic circuits. In power electronic systems, components that contribute predominantly to system failure are IGBTs/MOSFETs, diodes and capacitors. The reliability performance of these components are affected by environmental and stress factors. One of the documents that provides reliability data and modeling of power electronic components is the military handbook, MILHDBK-217F [139]. According to the MILHDBK-217F, the failure rates of these components are described as shown below.

4.5.5.1 Power electronic circuit components

Since the MILHDBK-217F military does not provide data for IGBTs, it was assumed that the estimation of failure rates of MOSFETs are applicable for IGBTs.
For switches (MOSFET/IGBTS), the failure rate is described by:

$$\lambda_{IGBT} = \lambda_{IGBT_b} \pi_T \pi_Q \pi_E \quad \text{Failures}/10^6 \text{ hours,} \tag{4.26}$$

where λ_{IGBT_b} is base failure rate of the IGBT, π_T temperature factor, π_Q quality factor and π_E environmental factor.

Similarly, failure rates of diodes are given by:

$$\lambda_{diode} = \lambda_{diode_b} \pi_T \pi_S \pi_C \pi_Q \pi_E \quad \text{Failures}/10^6 \text{ hours,} \tag{4.27}$$

where λ_{diode_b} is base failure rate of the diode, π_S voltage stress factor, π_C contact construction factor and π_T, π_Q and π_E are as for IGBTs.

Capacitor failure rate is given by

$$\lambda_{cp} = \lambda_{cp_b}\pi_T\pi_C\pi_V\pi_{SR}\pi_Q\pi_E \text{ Failures}/10^6 \text{ hours}, \tag{4.28}$$

where λ_{cp_b} is base failure rate of the capacitor, π_V voltage stress factor, π_{SR} series resistance factor and π_T, π_C, π_Q and π_E are as for IGBTs.

4.5.5.2 Reliability of PV Panels:

Reliability modeling of large systems such as PV systems with a large number of system components could result in a large number of system states and increase modeling complexity. Therefore, the equivalent MTTF and MTTR for subsystems are needed to drive an equivalent failure rate λ and repair rate μ. The availability of system components can be modeled as a Markovian with two states, *"up"* and *"down"* with known failure and repair rates. The PV panels are constructed from n parallel branches; each branch is constructed by connecting m series solar cells. The equivalent failure rate of a branch can be calculated by summing the failure rates of the m series solar cells. The failure of a solar branch leads to the failure of the PV panel. Thus, the availability and unavailability of PV panels can also be calculated using (4.22) and (4.23).

4.6 Reliability Modeling of PV system

In order to build a generation model for the entire PV system that consider both the effect of input variability and system components failures, two modeling steps are taken to build a generation model for PV system: (1) modeling the dependency of the output on the variability of the solar radiation and (2) the outage due to failure of system components (failure rate). These two models are then combined to produce a single generation model that can be viewed as a single source with multi-state. The blocks that constituted the model are depicted in Figure 4.5.

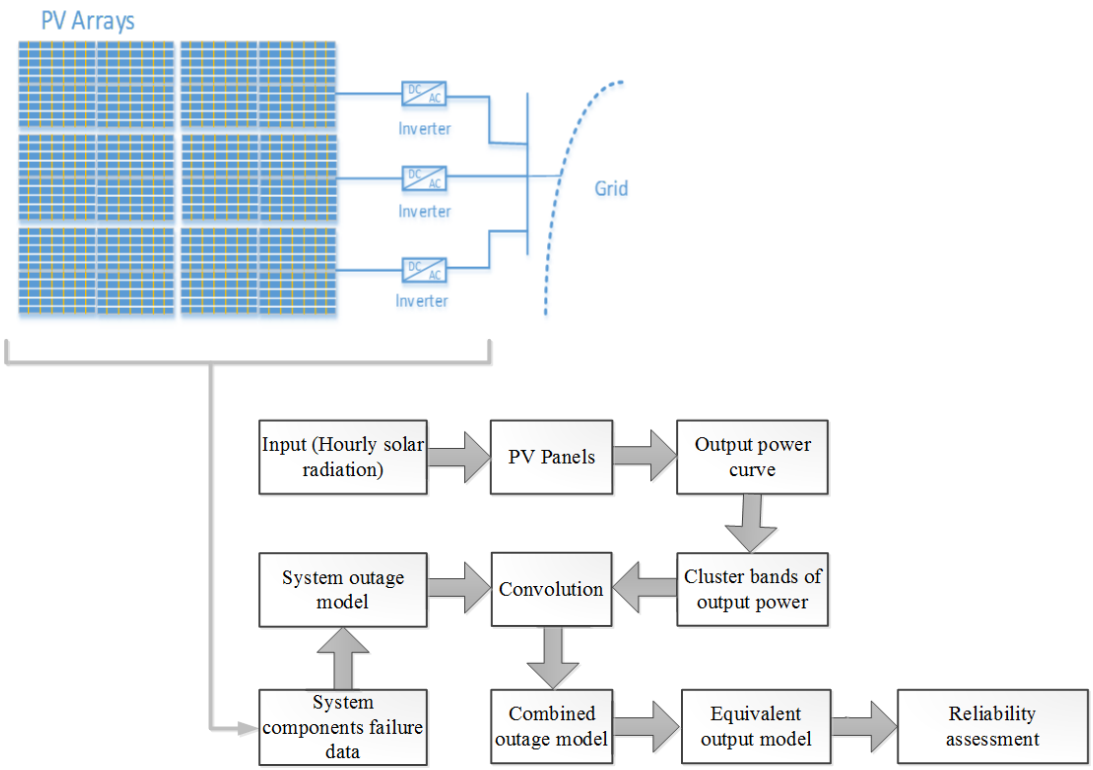

Figure 4.5 Model combining input variability and system component failures

The failures of the components a PV system are assumed independent events; availabilities of system components can also be modeled as Markovian components with two states, *"up"* and *"down"*. The assessment of the availability of the system output is addressed by separately modeling the independent failures of system components and the dependency on the input availability. The equivalent availability and unavailability of system components can be estimated by calculating the equivalent failure and repair rates. For each array, the

MTTF and MTTR for M components can be obtained. Each array can then be represented by equivalent MTTF and MTTR. The capacity outage probability and frequency table can be constructed for a PV farm with N arrays by adding new units sequentially to the table with the capacity model building approach explained in section 4.3. Based on the FOR of system arrays, the COPAFT of PV system can be built using the unit addition algorithm. This is a recursive algorithm that starts with the distribution of one unit (a PV array in this case) and successively convolves with it the distributions of the remaining units, one unit at a time. The steps of combining the viability model with the outage model are the same as explained in section 4.3.

4.7 Case Studies

The proposed method is applied on the IEEE RTS [140]. The parameters and structure of the PV system were taken from [39]. In this work, the solar radiation data for Santa Maria, CA region were taken from [127]. The data obtained from [127] for one year were utilized to estimate the output power of the PV system. In this work, the failure rates of system components were assumed as follows: for both DC/AC inverters and DC/DC converter are 0.000027 failures per hour, and for solar panels are 0.000011 failures per hour [141]. The repair rates of the DC/AC inverters and DC/DC converter were assumed 0.1 repair per hour. For the PV panel, the repair rate was assumed 0.2 repair per hour.

To validate the results, the reliability indices of IEEE RTS are calculated using Monte Carlo simulation and the results are shown in Table 4.9.

Table 4.9 Reliability Indices of the IEEE RTS With 100 MW PV Farm

Method	LOLP	EDNS (MW/yr)	LOEE (MWh/yr)	LOLF occ./yr	LOLE (hr/yr)
Base Case					
DC	0.001069	0.1348396	1181.195	2.01600	9.3688
PV Power Only					
Proposed	0.000795	0.097248	849.554	1.73463	6.9453
PV Power with Inclusion of (FOR)					
Proposed	0.0008259	0.1030553	900.2912	1.74285	7.2157
MCS	0.0008356	0.1030920	900.7016	1.74397	7.2998

DC: Discrete convolution; MCS: Monte Carlo simulation

Chapter 5

Capacity Value of Variable Energy Resources

Capacity value of VERs (or capacity credit) is an important metric used to assess the contribution of VERs to the adequacy of power system. The effective load carrying capability (ELCC) approach is commonly used to measure the capacity value of generating units [64]. The ELCC of a generating unit is measured by the amount of system load increase that gives the same LOLE index of the system (prior to adding a new generating unit) [64]. Traditionally, iterative process is required to measure the capacity value of a generating unit. In the process of calculating the capacity value, the system load is incremented across all hours using an iterative process by a step of ΔL, and reliability metrics such loss of load probability (LOLP) or loss of energy expectation (LOLE) are recalculated for every iteration until the predefined reliability target is met (i.e. the reliability target of the system before adding the new generation unit). However, this process is computationally expensive and time consuming especially for large and complex systems. In this work, direct, non-iterative method is developed to calculate the capacity value of VERs.

5.1 Reliability-Based Methods used to Calculate the capacity Value of VERs

Reliability based methods are considered the most robust in the assessment of the contribution of VERs to the generation adequacy assessment [142–144]. Reliability based methods use the reliability indices such as LOLP or LOLE as a criterion to determine the capacity value of VERs. There are several methods to calculate the capacity value of VERs using ELCC. These methods include; 1) effective load carrying capability, 2) equivalent conventional power, and 3) equivalent firm power. These methods and other methods, approximation methods, are briefly discussed in the following sections.

5.1.1 Effective Load Carrying Capability

The calculation of the capacity value of VERs using ELCC method requires building a generation model, COPAFT, and load model as explained in section 3.2. These two model are convolved to calculate system reliability indices. When VERs are added to the system, the COPFAT is reconstructed and convolved with system load model. The system load is then increased by a step of ΔL across all hours and the system indices such as LOLE index is recalculated until the same LOLE index prior adding the new generator is obtained. The capacity value of the addition generating unit is calculated as follows.

$$CV = \frac{\sum \Delta L}{G_c} \times 100\%, \tag{5.1}$$

where the CV is the capacity value of the new generating unit, G_c is the nameplate capacity of the new generating unit.

5.1.2 Equivalent Conventional Firm Power (ECFP)

The capacity value of VERs is defined as the capacity of a benchmark generation unit that resulting the same reliability indices when the VERs is added to the system [44, 45]. In this process, the benchmark unit is assumed to be perfectly reliable. The steps of calculating the capacity value using this approach are summarized as follows.

1. Add the output of VERs to the system.
2. Build COPAFT with VERS.
3. Convolve generation model with load model.
4. Calculate the LOLE index of the system.
5. Replace the VERs with a dispatchable unit (benchmark) with a capacity equal to the installed capacity of VERs.
6. Recalculate the LOLE index of the system.
7. Gradually reduce the capacity of the benchmark unit.
8. Repeat the step 7 until the LOLE index of the system after adding VERS is achieved.
9. The capacity of the benchmark unit that procedures the same LOLE index after adding VERS is the capacity value of VERs.

5.1.3 Equivalent Conventional Power (ECP)

The capacity value of VERs are calculated using the same steps as ECFP, except that the benchmark unit is assumed not perfectly reliable. The FOR of the benchmark unit is usually chosen to be small. The main difference between the ELCC approach and ECFP and ECP is that in the ECFP and ECP methods, the distribution of distribution of available capacity in a given hour change whereas ELCC method does not [44, 45, 145].

5.1.4 Approximation Methods

Calculation of the capacity value of VERs based on iterative methods tends to be computationally intensive due to the requirement of repetitive calculations. Several authors have proposed different methods to calculate the capacity value of VERs using non-iterative methods. Non-iterative methods are direct and computationally efficient, but often involve approximations. For instance, the method presented in [61] uses a graphical method to estimate the capacity value of wind power. The graphical method is based on using an exponential function to approximate the change in LOLE (loss of load expectation) resulting from an increase in load. Although the graphical method is computationally efficient, this approximation could lead to considerable errors [63]. The method presented in [62], the Z-method, uses the probability distribution of the generation reserve margin to calculate the capacity value of VERs. However, this method assumes that the probability distribution of the generation margin preserves its shape even after adding wind power [65]. Also, the methods presented in [61, 62] ignore the correlation between demand and wind power [65]. The non-iterative analytical method presented in [63] uses the concept of joint probability distribution to calculate the capacity value of VERs using effective load carrying capability (ELCC) approach considering the correlation between the load and the available output power of VERs. However, this method requires a pre-specified value for the LOLE index to be used to calculate the ELCC before and after adding VERs. Furthermore, as stated by the authors themselves [63], the accuracy of estimating the ELCC of the system relies on the chosen number of "i.e. coincidental demand-generation levels", and the optimal number of such levels that yields the best accuracy is difficult to determine.

5.2 A Direct Method to Calculate the Capacity Value of VERs

The ELCC is traditionally estimated using iterative processes where the system load across all hours is linearly incremented by a certain amount, usually a constant step, until the targeted reliability index reaches a specified level. However, this process is computationally expensive and time consuming especially for large systems. In the process of calculating the PLCC, if VERs are added to the system as load modifiers, the system load model is modified but the generation model remains unchanged. On the other hand, if VERs are added to the system as generating units, the generation model is modified and the load model remains unchanged. However, in the adequacy assessment, both approaches have been used to calculate the capacity value of VERs. After adding VERs, the generation reserve margin increases which leads to improvement in system reliability.

In this work, a direct method is proposed to calculate the capacity value of VERs using the ELCC as a criterion. The proposed method is based on the fact that the capacity value of VERs is bounded between 0 MW and their installed capacity (rated capacity). Also, it is assumed that the increase in system load is evenly distributed on the load profile, as has been commonly used [44, 45, 64]. Therefore, the capacity value can be calculated by augmenting the generation reserve margin by the maximum capacity of VERs. The augmented reserve margin model can be expressed in terms of generation, load, and VER models using (3.8) and (3.9) as follows.

$$M_{au} = M + C_V, \tag{5.2}$$

where M is the generation reserve margin prior to adding VERs and C_V is the available capacity of VERs.

The CDF of the augmented margin, CDF_{au}, is created in same manner as creating a CDF for the original margin. However, the range of the augmented reserve margin is from $-L$ to C_R rather than ranging from $-L$ to 0 as in the original system (prior to adding VERs), where C_R is the maximum capacity of the VER. A typical CDF of an augmented margin is shown in Fig. 5.1. The CDF of the generation reserve margin of the original system crosses the zero level at $P(0)$. Since the capacity value is defined as the amount of load increase (after adding VERs) that would return a reliability index to its initial value (prior to adding VERs), the capacity value of a VER can be determined by projecting $P(0)$ to the augmented margin. In other words, the capacity value of a VER can be directly calculated by projecting the point at which the CDF of the augmented margin meets the level of reliability index before adding VERS to the system as shown in Fig. 5.1. Mathematically, the capacity value of VERs can be determined as follows.

$$\text{Capacity Value} = M_{au}\{X : \text{CDF}_{au}(X) = P(0)\}, \tag{5.3}$$

where $\text{CDF}_{au}(X)$ is the cumulative probability of X MW of the CDF of the augmented reserve margin.

The general procedure of the proposed method for calculating the capacity value is given as follows.

1. Construct probability distributions of conventional generators, loads, and output power

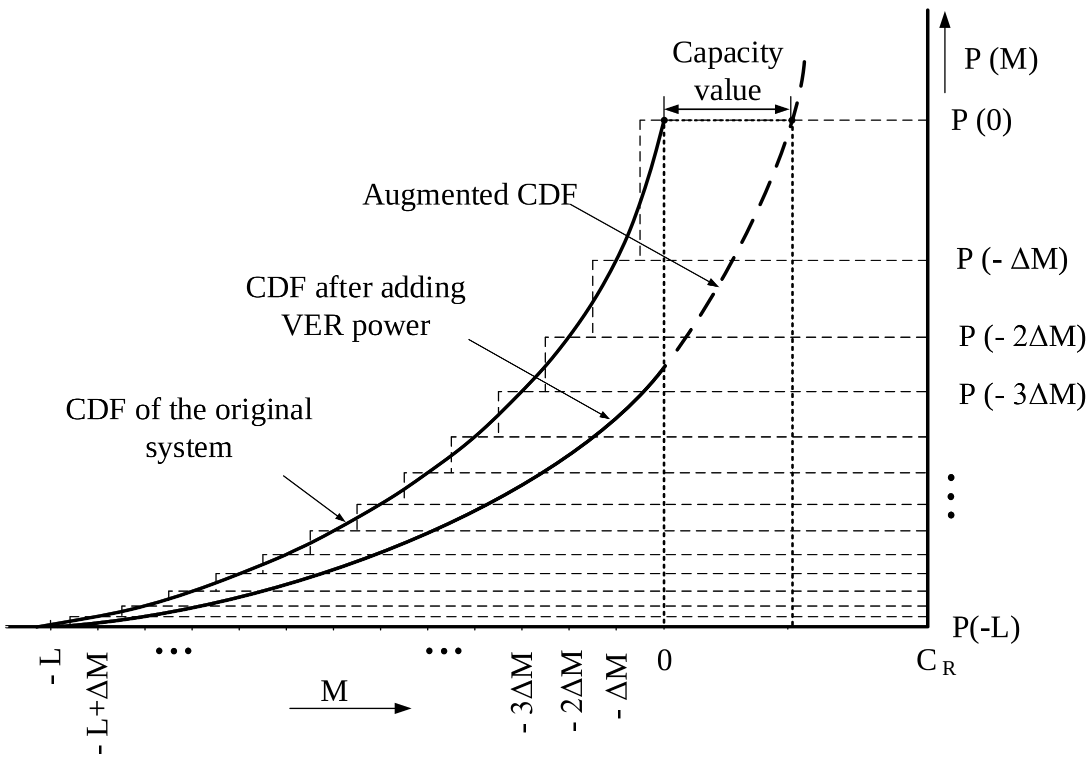

Figure 5.1 Cumulative distribution function of an augmented margin before and after adding VERs

of VERs with and without including their forced outage rates.

2. Use discrete convolution to determine the margins for: (1) the original system, (2) the system after adding the output power of VERs, and (3) the system after adding the output power of VERs and considering their forced outage rates.

3. Adjust the new margins (after adding the power of VERs) by augmenting these margins by the rated installed capacity of the VERs.

4. Determine the reliability indices of the original system. Determine the points at which the new margins (after adding the power of VERs) intersect with these indices. These points represent the capacity value.

5.3 Case Studies

The proposed method is applied on the IEEE reliability test system (IEEE RTS) [123]. The output of VERs is modeled as described in section 4.3. In this paper, a wind farm with 150 MW (50 WTGs $\times$ 3 MW) capacity is added to the system assuming that all WTGs are identical. In the case studies reported below, two wind data sets are used: data set A [128] and data set B [146]. For convenience, these are referred to as Farm A and Farm B. The reason of choosing these data sets is to determine the effect of the correlation between the output power of wind farms and load profile on the reliability indices and the capacity values. The correlation coefficients between these data sets and the load profile of the IEEE RTS are as follows: -0.1059 for Farm A and 0.0686 for Farm B.

A typical wind turbine characteristic is used (type Vesta V90-3.0 MW [124]; rated power: 3 MW; rated, cut-in, and cut-out speeds: 15 m/sec, 3.5 m/sec, and 25 m/sec respectively). In the cases reported here, the impact of different values of forced outage rates of WTGs and wake effect on the capacity values of wind farms are studied. The reliability data of WTGs are given in Table 4.1. The failure rates and mean time to failure (MTTF) shown here lie in the ranges for actual WTGs, as reported in [125]. Repair times are calculated from the FORs and failure rates of WTGs and are expressed in terms of mean time to repair (MTTR).

5.3.1 Capacity Value of Wind Farm–Forced Outages and Wake Effect

In this section, the well-known reliability indices and the capacity value of the wind Farm A are calculated. Grid scale wind farms are constructed from a large number of WTGs, and the variation of the output of WTGs within the farm depends on several factors including the wake effect [14]. Due to the wake effect, the downstream (with respect to the direction of the wind) WTGs generate less power than the upstream WTGs because they are exposed to lower wind speed. Several methods have been proposed in the literature to model the wake effect and to evaluate the resulting losses in the output power of wind farms [147, 148]. In this work, system advisor model (SAM) [149] is used to consider the output variation of WTGs due to the wake effect in evaluating the capacity value of wind power. Two factors are considered in calculating the capacity value and reliability indices as following: (1) forced outages of WTGs and (2) wake effect .

5.3.1.1 Capacity Value of Wind Power Considering the Forced Outages of WTGs

In this case study, the impact of forced outages of WTGs on the capacity value of wind power is evaluated by considering different FORs of WTGs. In this work, the capacity value of wind power is evaluated for four different case studies. The forced outage rates of WTGs are considered as follows. *Case 1*: 0.0, *Case 2*: 0.04, *Case 3*: 0.08, *Case 4*: 0.12. In all of these cases, the wake effect is ignored. System indices and capacity values of wind power for the these cases are given in Table 5.1. For each case study, the capacity value is calculated by taking the LOLE and the LOLF indices as criteria as shown in the last two columns of Table 5.1. The first row of Table 5.1 represents the base case (prior to adding wind power).

5.3.1.2 Capacity Value of Wind Power Considering the Wake Effect

In this case study, the capacity value of wind power is evaluated considering the wake effect with different values for the forced outage rates of WTGs. Four case studies are performed

Table 5.1 Reliability Indices and Capacity Value–150 MW Wind Farm A Considering the Effect of Different FORs of WTGs

	LOLP	EPNS (MW)	LOLF (occ./yr)	LOLE (h/yr)	Capacity Value (%) LOLE	LOLF
Base case	0.001072	0.13520	2.01582	9.3681	–	–
Case 1	0.000799	0.09573	1.55870	7.0059	26.67	24.67
Case 2	0.000821	0.09721	1.61347	7.1969	25.33	24.00
Case 3	0.000830	0.09862	1.63284	7.2778	23.33	22.00
Case 4	0.000839	0.09990	1.64435	7.3549	22.67	20.67

considering the wake effect with different forced outage rates of WTGs as follows. *Case 1*: 0.0, *Case 2*: 0.04, *Case 3*: 0.08, and *Case 4*: 0.12. System reliability indices and capacity values of wind power for the four cases are given in Table 5.2. For each case study, the capacity value is calculated by taking the LOLE and the LOLF indices as criteria as shown in the last two columns of Table 5.2.

Table 5.2 Reliability Indices and Capacity Value–150 MW Wind Farm A Considering the Wake Effect and Different FORs of WTGs

	LOLP	EPNS (MW)	LOLF (occ./yr)	LOLE (h/yr)	Capacity Value (%) LOLE	LOLF
Case 1	0.000992	0.123285	1.91430	8.6945	20.00	18.67
Case 2	0.001001	0.124471	1.92040	8.7704	18.66	17.68
Case 3	0.001011	0.125668	1.93530	8.8538	18.00	16.67
Case 4	0.001021	0.126872	1.94617	8.9176	17.00	15.33

As it is expected, the results given in Table 5.1 and Table 5.2 show that the addition of a wind farm improves the reliability of the system. They also show that as the value of FOR increases, the reliability and the capacity value of the system deteriorates. In addition, when both wake effect and forced outages of WTGs are considered, the capacity value of wind power decreases.

5.3.2 Effect of Correlation

To investigate the effect of correlation between wind speed and load demand on the capacity value of wind power, wind Farm B is added to the IEEE RTS and the results are compared with case of wind farm A. For simplicity and to avoid repetition, only the forced outage rate of 0.08 is used in this section to calculate reliability indices and the capacity value of wind Farm B. Three case studies are considered as follows. *Case 1*: ignore both wake effect and forced outages of WTGs, *Case 2*: consider wake effect and ignore the forced outages of WTGs, *Case 3*: consider both wake effect and forced outages of WTGs. The results of these case studies are given in Table 5.3.

Table 5.3 Reliability Indices and Capacity Value–150 MW Wind Farm B

	LOLP	EPNS (MW)	LOLF (occ./yr)	LOLE (h/yr)	Capacity Value (%)	
					LOLE	LOLF
Case 1	0.000673	0.080620	1.41762	5.9053s	32.00	26.00
Case 2	0.000757	0.093128	1.54557	6.6349	30.66	25.33
Case 3	0.000915	0.113578	1.84227	8.0132	28.66	22.00

To show the effect of the correlation between the output power of wind farms and the load profile on the reliability indices and capacity values, compare Case 1 of Table 5.3 with Case 1 of Table 5.1, Case 2 of Table 5.3 with Case 1 of Table 5.2, and Case 3 of Table 5.3 with Case 3 of Table 5.2. By comparing these results, it can be seen that a positive correlation between wind speed and load profile contributes to a higher capacity value of wind power and improvement in system reliability.

5.3.3 Capacity Value of VERs Versus Penetration Levels

The proposed method can also be used to easily determine the optimal capacity to install at a location selected for a wind farm. Since the proposed method requires only one solution for every candidate installed capacity, it is easy to determine the optimal capacity value. In this work, data of Farm B is used and the capacity values are calculated for different penetration levels as shown in Fig 5.2.

Four case studies are implemented as follows: (1) using the LOLP index as a criterion and neglecting the forced outages, (2) using the LOLP index as a criterion and considering the forced outages, (3) using the LOLF index as a criterion and neglecting the forced outages, and (4) using the LOLF index as a criterion and considering the forced outages. It can be seen from the curves of Fig. 5.2 that as the penetration level increases, the capacity value of wind power also increases and then starts decaying as the penetration level is further increased. This analysis allows the planner to determine the penetration level that results in a maximum capacity value to allocate the cost of a project.

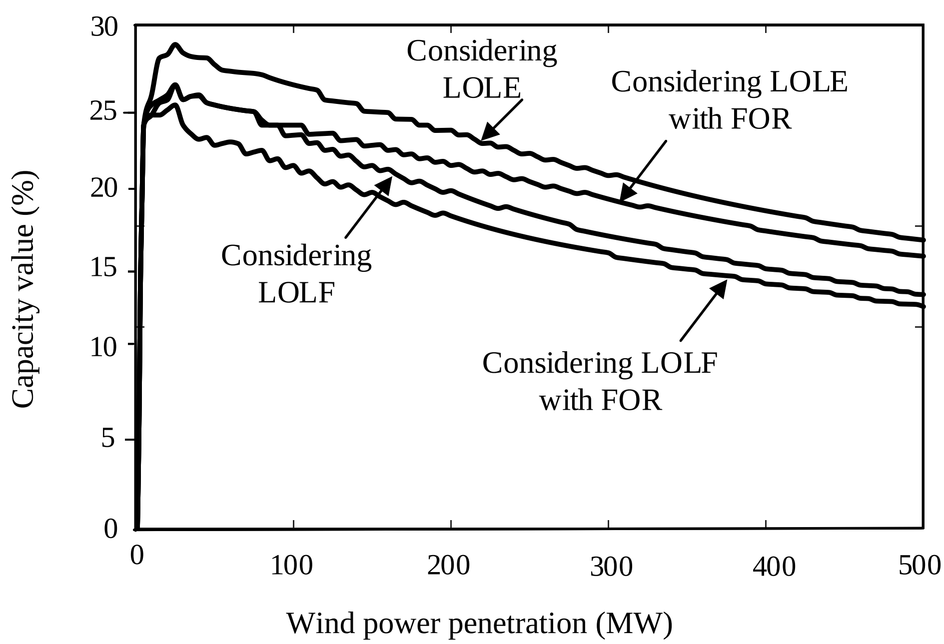

Figure 5.2 Capacity value of wind power as a function of penetration level

5.3.4 Validation of Proposed Method

The proposed method is validated by comparing the results obtained by the method with those obtained using an iterative method. The two methods are used to calculate the capacity value of wind Farm A for *Case 1* and *Case 2* (with and without considering the forced outages of WTGs and neglecting the wake effect). Using the proposed method, the results of *Case 1* and *Case 2* are shown in Fig. 5.3. The capacity value of the wind farm is 40 MW and 38 MW in cases of neglecting and considering the forced outages of WTGs respectively.

The iterative ELCC method is used to calculate the capacity value of wind farm A by increasing the loading level of the system by ΔL until the reliability level (prior to adding wind power) is reached, which is in this case the LOLE index. The results are shown in Fig. 5.4 which are identical to those calculated using the proposed method.

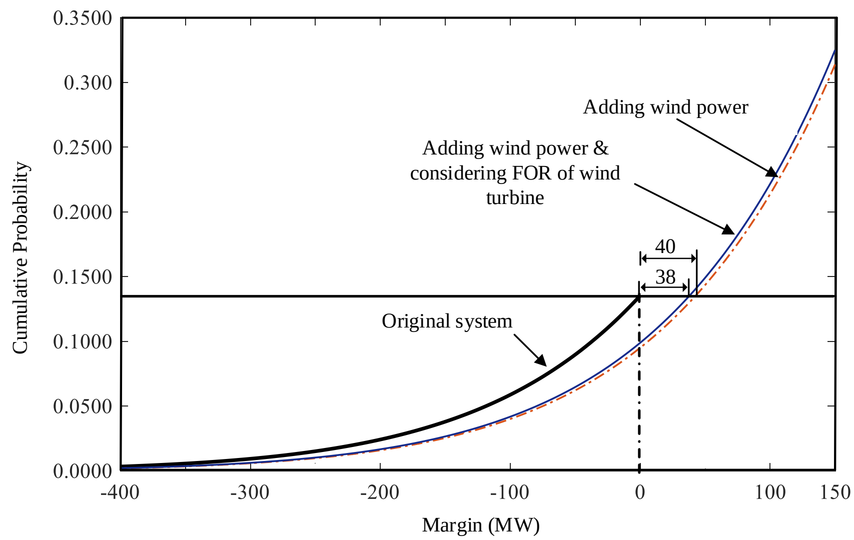

Figure 5.3 Capacity value of wind power using the proposed method

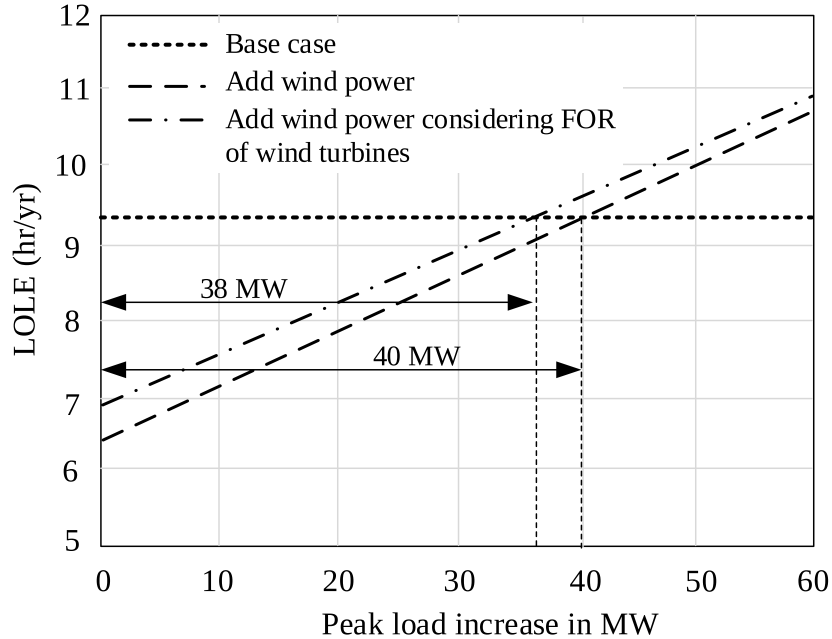

Figure 5.4 Capacity value of wind power as function of peak load increase using iterative method

It can be seen from Fig. 5.3 that the proposed method is able to calculate the capacity value using only one iteration compared to the capacity value calculated using the iterative method shown in Fig. 5.4. It is also clear that the capacity value of wind power is less when the FORs of WTGs are considered which is not surprising.

Chapter 6

Quantification of Storage Necessary to Firm Up Wind Generation

The integration of energy storage systems with intermittent sources has become a practical solution to overcome these challenges. This is largely because of the rapid growth in deployment and improved technology of energy storage systems. A method for quantifying the size of energy storage systems to meet specified reliability targets was proposed by Mitra in [89, 90]. This work extends this method to quantify the size of the required energy storage to firm up wind power and improve system reliability to a specific target. In this work, the effect of the input variation (wind speed) on the output power of wind turbine generators (WTGs), forced outages of generating units including WTGs, and other factors (e.g., transmission capacity and power quality constrains) are included. Correlation between wind generation and load demand is also considered. Taking into consideration the above factors, the proposed method determines the amount of storage required to firm up the generation from the wind farm that is added, so as to provide the same reliability level as a conventional (dispatchable) generating unit of the same nameplate capacity as the wind farm. System reliability enhancement, in terms of reliability indices, is also assessed with respect to wind farm location and the energy storage. Metrics commonly used for reporting bulk power system reliability are utilized in this work: loss of load probability (LOLP), expected demand not supplied (EDNS), loss of load frequency (LOLF), and mean down time

(MDT). However, this paper addresses the matter of size only; it is up to the planner to select a suitable technology based on cost and other considerations.

6.1 Energy Storage System

This section presents a method for determining the size of the energy storage that is required to increase the available energy at wind farm locations. Due to transmission line capacity limits and operational constraints, and the uncertainty associated with the overall energy production of wind farms, the output power of a wind farm that is available to the system could be lower than its nameplate capacity. In fact the output variations depend upon several factors such as geographic location, number of WTGs on the farm, differences between WTGs, turbulence and wake effects, and terrain effects [111, 150]. The accuracy of modeling the output power of WTGs also varies with time scales (the frequency of wind speed observation intervals can be 5 minutes, 10 minutes, hourly, etc.). Further, it has been reported that the error in estimating annual energy production of wind power can be up to 12% [150, 151]. Moreover, failures of WTGs have a significant impact on the available power. Thus, in determining the energy storage size, such uncertainty factors should also be considered.

6.1.1 Energy Storage Sizing

The proposed method of quantifying the size of the energy storage is based on previous work presented in [89, 90]. Consider a wind-integrated power system that provides supply of availability ρ_0 to the system load. Now consider that part of the load curtailment, P_L, that can be directly attributed to the variability of wind power. This quantity can be determined from the difference between the nameplate capacity and the capacity value of the wind farm. The capacity value is the amount of load the wind farm can reliably support, given the variability of wind. Firming the wind output consists of adding a storage system that is sufficient to increase the availability of supply to ρ_1, which is what would be available if there were firm (dispatchable) generation instead of wind. Thus, the power capacity of the required storage unit should be at least P_L. The energy capacity can then be determined as follows.

Define the unavailability reduction ratio α as [89]:

$$\alpha = \frac{1 - \rho_1}{1 - \rho_0}. \tag{6.1}$$

The unavailability reduction ratio can be understood thus: suppose that $\rho_0 = 0.999$ and that it is required to increase the availability by an additional "9," i.e., to $\rho_1 = 0.9999$; then, $\alpha = 0.1$.

Now assume that the storage system that will improve the system reliability to ρ_1 can sustain a load of P_L for time t_A. Then, service interruption occurs when the grid supply is down and the storage has been depleted. The probability of this event can be described by (6.2).

$$\begin{aligned} P\{L_s\} &= P\{\{R > t_A\} \cap L_{\bar{s}}\} \\ &= P\{R > t_A \mid L_{\bar{s}}\} P\{L_{\bar{s}}\} \\ &= \left(\int_{t_A}^{\infty} f_R(r) dr \right) P\{L_{\bar{s}}\}. \end{aligned} \tag{6.2}$$

The variables in (6.2) are defined as follows [89].

$L_{\bar{s}}$: event that the load is curtailed in the absence of storage;

L_s: event that the load is curtailed in the presence of storage;

R: random variable representing the down time (outage duration);

$f_R(r)$: probability density function of R.

In (6.2), $P\{L_s\}$ is clearly $1-\rho_1$, and $P\{L_{\bar{s}}\} = 1-\rho_0$. From (6.1) and (6.2), it is clear that

$$\int_{t_A}^{\infty} f_R(r)dr = \alpha. \tag{6.3}$$

The solution to (6.3) can be obtained analytically for simple systems [89], but for more complex systems it is more convenient to use (6.4), which has been shown to be equivalent to (6.3) [90].

$$\int_0^{t_A} r f_R(r)dr = (1-\alpha)\bar{r} \tag{6.4}$$

The solution to (6.4) can be easily obtained from interruption time statistics generated by using sequential Monte Carlo simulation. Suppose the interruption durations without the storage system are arranged in order of increasing magnitude. If $\bar{r}$ is the mean interruption duration (given by the mean of *all* interruption durations), then that time for which the mean of all equal and shorter interruptions is closest to $(1-\alpha)\bar{r}$ gives the estimate of t_A.

Equation (6.4) represents the basic relation that quantifies the required energy capacity of the storage system. However, the storage unit itself may not be perfectly reliable. In order to compensate for this, the storage device should have an energy capacity that enables it to provide the required power (P_L) for a period of time (t_S) that is given by (6.5) [89,90].

$$t_S = \frac{t_A}{A_S}, \tag{6.5}$$

where A_S is the availability of the storage system. Therefore, the power capacity of the selected storage unit should be at least P_L, and the energy capacity should be at least $P_L t_S$.

In wind power planning projects, the errors associated with wind power prediction can lead to significant challenges for system planners and operators. Also, wind speed varies with both time and location. For these reasons, wind integration studies are generally conducted prior to the development phase of wind power projects to assess these impacts. With regard to storage system planning projects, several authors have discussed the effect of wind power prediction error on sizing energy storage systems [151–154]. Therefore, the available statistical data of wind power may not accurately reflect the long term variation of wind speed [150,151,155]. Thus, in the planning phase, additional power may be required to compensate for the long term error associated with wind energy production and estimation. In this work, the additional power of energy storage system P_{ESS} can be calculated as follows.

$$P_{ESS} = P_L(1 + \gamma), \tag{6.6}$$

where γ is the anticipated long term error associated with wind energy production and estimation.

6.1.2 Energy Storage Operation

In order to evaluate the effect of adding an energy storage device with a rated power of P_{ESS} on the reliability of the system, the following operation constraints are considered [70]:

$$0 \leq P^i_{dis}(t) \leq P^i_r \quad \text{for} \quad t \in [0, T], i = 1, 2, \ldots, N_b, \tag{6.7}$$

where T is the period of the study, $P_{dis}^i(t)$ is the discharging power of the energy storage device at bus i at time t in MW, and P_r^i is the rated power of the energy storage system at bus i in MW.

$$0 \leq P_{chr}^i(t) \leq P_r^i \quad \text{for} \quad t \in [0, T], i = 1, 2, \ldots, N_b, \tag{6.8}$$

where $P_{chr}^i(t)$ is the charging power of the energy storage system at bus i at time t in MW.

The inequalities (6.7) and (6.8) constrain the charging and discharging power to remain within the power rating of the energy storage system. The energy constraints of the storage system are imposed by (6.9).

$$0 \leq En^i(t) \leq En_r^i \quad \text{for} \quad t \in [0, T], i = 1, 2, \ldots, N_b, \tag{6.9}$$

where $En^i(t)$ and En_r^i are the energy state of charge and the energy rating of the storage system respectively at bus i in MWh. The energy state of charge of the storage system can be expressed as follows.

$$En^i(t+1) = En^i(t) - \frac{1}{\eta_{dis}} P_{dis}^i(t) + \eta_{chr} P_{chr}^i(t),$$

where η_{chr} and η_{dis} are the charging and discharging efficiencies of the storage system respectively.

In the literature, several authors have proposed different operation strategies for energy storage systems [69, 156, 157]. In this work, time-shift technique is applied as described in [69]. The state of charge and discharge of the storage system is represented by means of logic states (i.e., 1 for discharging and 0 for charging). The discharging states represent the hourly down-time statistics of wind power. In the simulation process, the available wind power is evaluated based on the temporal resolution of wind data and the discharging and charging capacities are determined accordingly.

6.1.3 Approach for Reliability-Based Storage Sizing

Fig. 6.1 provides an overview of the steps employed in the proposed approach. Reliability evaluation is performed by seeking dispatch solutions that minimize system curtailment, considering wind power uncertainty, forced outages of generation units including WTGs, and system operations constraints (power balance, generation and transmission capacites, and power quality constraints). Details of this model are provided in the next section.

6.2 Network Modeling And Reliability Evaluation

In composite reliability evaluation studies, repetitive solutions of an optimization problem with an objective function of minimum load curtailment are performed. This section describes the formulation and incorporation of the objective function of minimum load curtailment using nonlinear programming and the AC power flow model. Sequential Monte Carlo simulation is used to emulate the behavior of the system and estimate system reliability indices. This consists of sequential assessments of the reliability of the states that the system assumes in successive time steps over the planning horizon. For each such state, the objective is to determine a dispatch that minimizes the load curtailment, subject to the equality constraints of power balance, the inequality constraints of equipment capacity and power quality, and the availability of system components. In this section, the details of system modeling and reliability evaluation are described.

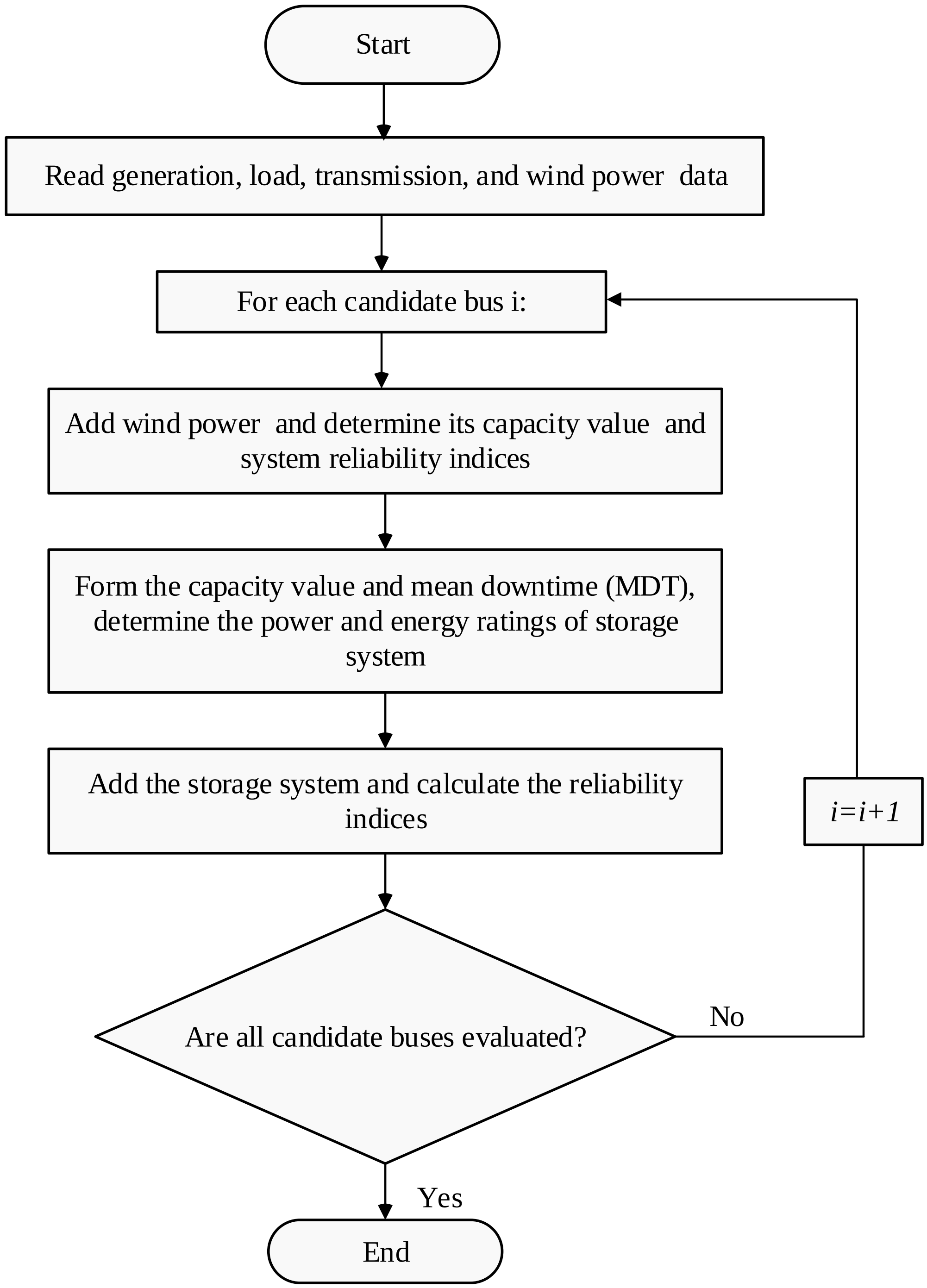

Figure 6.1 General procedure for reliability-based storage sizing

6.2.1 System Modeling

For each hour, the system state is defined by the component states and capacities. The output of wind power is determined by the corresponding wind turbine states and hourly output power. Then a feasible dispatch is sought by solving the following minimization problem [158].

$$\text{Loss of Load} = \min\left(\sum_{i=1}^{N_b} C_i\right) \tag{6.10}$$

subject to

$$\begin{aligned}
&P(V,\delta) - P_D + C = 0\\
&Q(V,\delta) - Q_D + C_Q = 0\\
&P_G^{min} \le P_G \le P_G^{max}\\
&Q_G^{min} \le Q_G \le Q_G^{max}\\
&V^{min} \le V \le V^{max}\\
&|F(V,\delta)| \le F^{max}\\
&\delta \quad \text{unrestricted}
\end{aligned} \tag{6.11}$$

where C_i is the load curtailment at bus i, C is the vector of load curtailments $(N_b \times 1)$, C_Q is the vector of reactive load curtailments $(N_b \times 1)$, V is the vector of bus voltage magnitudes $(N_b \times 1)$, δ is the vector of bus voltage angles $(N_b \times 1)$, P_D and Q_D are the vectors of real and reactive power loads $(N_b \times 1)$, P_G and Q_G are the vectors of real and reactive power outputs of the generators $\left(N_g \times 1\right)$, P_G^{min}, P_G^{max}, Q_G^{min} and Q_G^{max} are the vectors of real and reactive power limits of the generators $\left(N_g \times 1\right)$, V^{max} and V^{min} are the vectors of maximum and minimum allowed voltage magnitudes $(N_b \times 1)$, $F(V,\delta)$ is the vector of power flows in the lines $(N_t \times 1)$, F^{max} is the vector of power rating limits of the transmission lines $(N_t \times 1)$, and $P(V,\delta)$ and $Q(V,\delta)$ are the vectors of real and reactive power injections $(N_b \times 1)$. In the foregoing, N_b is the number of buses, N_t is the number of transmission lines, and N_g is the number of generators.

The above model implies that for any encountered scenario (generation and transmission availability and load state) power will be routed through the network in such a manner as to minimize the system load curtailment.

6.2.2 Calculation of Reliability Indices

In order to capture interruption times and temporal relationships such as state of charge of the storage system, all indices are determined from sequential Monte Carlo simulation [159].

6.2.2.1 Mean down time (MDT)

The MDT is the average interruption duration, denoted by $\bar{r}$ earlier in this section. By definition,

$$\text{MDT} = \bar{r} = \int_0^{\infty} r f_R(r) dr \tag{6.12}$$

where the variables are as defined in (6.2). From the simulation, MDT is estimated using

$$\text{MDT} = E\left[\hat{r}\right]; \quad \hat{r} = \frac{1}{N_c} \sum_{i=1}^{N_c} T_{dn}^i \tag{6.13}$$

where $E\left[\cdot\right]$ is the expectation operator, $\hat{r}$ is the estimator of MDT, T_{dn}^i is the duration of ith interruption encountered during the sequential simulation, and N_c is the number of *cycles* simulated. A cycle consists of a service period T_{up}^i and an interruption period T_{dn}^i; the ith *cycle time* T_c^i equals $T_{up}^i + T_{dn}^i$. The total period of simulation T is given by $T = N_c T_c = N_c \left(T_{up}^i + T_{dn}^i\right)$.

6.2.2.2 Loss of load probability (LOLP)

The LOLP index can be estimated as follows.

$$\text{LOLP} = E\left[\Pi\right]; \quad \Pi = \frac{1}{T}\sum_{i=1}^{N_c} T_{dn}^{i} \tag{6.14}$$

where Π is the estimator of LOLP and the other variables are as defined above.

6.2.2.3 Loss of load frequency (LOLF)

The LOLF index gives the frequency of service outage and can be estimated as follows.

$$\text{LOLF} = E\left[\Phi\right]; \quad \Phi = \frac{N_c}{T} \tag{6.15}$$

where Φ is the estimator of LOLF and the other variables are as defined above. It should be noted that the unit of LOLF is failures per unit time; hence, if time is tracked in hours, (6.15) will yield LOLF in f/h, and may need to be converted into f/y, which is the customary unit for expressing LOLF. Also, LOLF is related to LOLP and MDT as follows.

$$\text{LOLF} = \frac{\text{LOLP}}{\text{MDT}} \tag{6.16}$$

6.2.3 Expected demand not supplied (EDNS)

The EDNS index is the sum of the products of probabilities of failure states and the corresponding load curtailments which can be calculated as follows.

$$\text{EDNS} = \sum_{x_i \in X_f} P\{x_i\} \times C\{x_i\} \tag{6.17}$$

where $P\{x_i\}$ and $C\{x_i\}$ are the probability of occurrence of state x_i and the system load curtailment in state x_i, and X_f is the set of failure states.

Using sequential simulation, EDNS is estimated from

$$\text{EDNS} = E\left[\hat{d}\right]; \quad \hat{d} = \frac{1}{T}\sum_{i=1}^{N_C} T_{dn}^{i} C\{x_i\} \tag{6.18}$$

where $\hat{d}$ is the estimator of EDNS and $C\{x_i\}$ is the minimum curtailment obtained from the solution of (6.10) for the prevailing state.

6.2.4 Stopping Criterion

In using Monte Carlo simulation to estimate power system reliability indices, a convergence criterion should be applied to stop the algorithm if there is not much change in the reliability indices. In this work, the stopping criterion is applied on the reliability indices as follows.

$$COV = \frac{\sqrt{Var(\rho_{N_c})}}{E\left[\rho_{N_c}\right]} \leq \varepsilon, \tag{6.19}$$

where COV is the coefficient of variation, $Var(\cdot)$ is the variance function, ρ_{N_c} is the value of the estimate of the reliability index of interest (such as LOLP or EDNS) at the end of N_c cycles, and ε is a pre-specified tolerance.

At intervals of several cycles, the COV is calculated. If this amount is less than or equal to the specified tolerance ε, the algorithm is terminated; otherwise, the simulation continues.

6.3 Case Studies

The proposed formulation is applied on the IEEE reliability test system (IEEE-RTS) [140]. The single line diagram of this test system is shown in Fig. 4.4. The load profile of the IEEE-RTS is used to calculate the hourly load of each bus in the system for a year. For the base case of the IEEE-RTS, the LOLP, LOLF, and EDNS indices are 0.001538, 2.695 f/y, and 0.20151 MW/y respectively.

In this study, a wind farm with 200 MW capacity is added to the system at the load buses assuming that all WTGs are identical (100 WTGs with nameplate capacity of 2 MW each). Actual observed wind speed data sets are used to calculate the output of WTGs. In the following case studies, three wind speed data sets are used to evaluate the effects of different correlation between the wind power and the load profile, and different temporal resolutions on the system reliability indices: *data set A* [126], *data set B* [160], and *data set C* [128]. The wind speed data sets are utilized to calculate the output of WTGs using equations (4.1) and (4.2).

A typical wind turbine characteristic is assumed (type Vesta V90-2.0 MW [124]). The reliability data of the WTGs are as follows: The mean time to failure (MTTF) and mean time to repair (MTTR) are 3600 h and 150 h respectively [81]. The MTTF lies in the ranges of actual WTGs, as reported in [125]. The MTTR is calculated from the forced outage rates and MTTF of WTGs. The case studies are summarized as follows:

1. Evaluating the effect of the temporal resolutions of the wind speed on system reliability: Due to unavailability of wind speed data for the same site with different temporal resolutions, the effects of correlation and temporal resolution on the system reliability indices are evaluated using three different wind speed data sets for different sites. Three different

case studies are considered. These case studies are not intended to compare the results; rather, they illustrate the impact of considering such factors on the planning decisions. In an actual planning study, comparisons should be conducted for wind speed data with different temporal resolutions, at the site under consideration.

2. Energy storage sizing: The proposed method (as explained in section 6.1) is used to determine the power and energy capacities required to firm up the generation from the wind farm that is added, so as to provide the same reliability level as a conventional (dispatchable) generating unit of the same nameplate capacity as the wind farm.

6.3.1 Wind Farm Locations and System Reliability

The selection of wind farm location usually depends on several factors such as wind availability, access to the grid, economic aspects, and reliability enhancement of the grid. In this work, the wind farm candidate locations are evaluated based on how much reliability benefit they can bring to the system i.e., by the extent to which a wind farm at a candidate location reduces the system EDNS. The following three cases are studied:

1. Case study 1: IEEE-RTS reliability indices with wind farm, assuming *wind speed data set A.*

2. Case study 2: IEEE-RTS reliability indices with wind farm, assuming *wind speed data set B.*

3. Case study 3: IEEE-RTS reliability indices with wind farm, assuming *wind speed data set C.*

The temporal resolutions of the wind speed data sets are as follows: (1) wind speed data set A has a temporal resolution of one hour, (2) wind speed data set B has a temporal resolution of 5 minutes, and (3) wind speed data set C has a temporal resolution of 10 minutes. The correlation coefficients between these data sets and the load profile of the IEEE-RTS are as follows: (1) -0.002 for data set A, (2) 0.0686 for data set B, and (3) -0.1059 for data set C. Whereas data set A and the load are almost uncorrelated, data set B has positive correlation and data set C has negative correlation with the load. For each case study, the wind power is connected to the load buses and then the reliability indices are calculated. System reliability indices for different wind locations are listed in Table 6.1, Table 6.2, and Table 6.3. Buses 21–24 do not have load and are not considered.

The entries in the tables may be understood thus. *Each row represents a separate study wherein a 200 MW wind farm as described above is added to the IEEE-RTS at the indicated bus, and the system EDNS, LOLP, LOLF and MDT are evaluated.*

Table 6.1 System Reliability Indices for IEEE RTS with 200 MW Wind Power Added at Different Buses: Data Set A

Wind Power at Bus No.	LOLP	EDNS (MW/y)	LOLF (f/y)	MDT (h)
1	0.001054	0.135182	3.079	3.00000
2	0.001071	0.137305	3.120	3.00641
3	0.001114	0.142770	3.228	3.02261
4	0.001122	0.143889	3.240	3.03302
5	0.001143	0.147287	3.285	3.04749
6	0.000988	0.125983	2.892	2.99239
7	0.001517	0.198447	2.639	5.03714
8	0.001201	0.155500	3.467	3.03375
9	0.001038	0.133087	3.042	2.99047
10	0.001025	0.131022	3.012	2.98240
13	0.000950	0.121135	2.770	3.00578
14	0.001161	0.149592	3.341	3.04280
15	0.001185	0.153112	3.418	3.03686
16	0.001011	0.128986	2.955	2.99695
18	0.000938	0.119248	2.737	3.00110
19	0.001032	0.132050	3.020	2.99238
20	0.001209	0.156707	3.496	3.02918

Table 6.2 System Reliability Indices for IEEE RTS with 200 MW Wind Power Added at Different Buses: Data Set B

Wind Power at Bus No.	LOLP	EDNS (MW/y)	LOLF (f/y)	MDT (h)
1	0.000991	0.120629	1.960	4.42908
2	0.001007	0.122628	1.974	4.46960
3	0.001047	0.127766	2.036	4.50344
4	0.001055	0.128817	2.054	4.50049
5	0.001078	0.132020	2.083	4.53337
6	0.000919	0.112048	1.814	4.43826
7	0.001496	0.195424	2.601	5.03883
8	0.001137	0.139781	2.204	4.51906
9	0.000971	0.118663	1.915	4.44386
10	0.000954	0.116734	1.878	4.45101
13	0.000887	0.107531	1.773	4.38240
14	0.001094	0.134194	2.122	4.51602
15	0.001120	0.137520	2.157	4.54845
16	0.000937	0.114838	1.860	4.41344
18	0.000876	0.105768	1.749	4.38536
19	0.000963	0.117694	1.894	4.45565
20	0.001147	0.140924	2.223	4.51867

The best candidate buses are determined by tracking system reliability improvement with respect to wind power location. Of the indices reported, the EDNS most effectively reflects the extent to which customers are affected by system outages. Therefore, the EDNS index is chosen to determine the best candidate buses to connect the wind farm at. The candidate buses are ranked based on the improvement of the system EDNS index (highest to smallest). In general, system reliability indices improve when wind power is added to the system in every case study which is not surprising. Overall, the system is found to benefit the most from installing the 200 MW wind farm at bus 18, 13, 6, 10 or 9.

Table 6.3 System Reliability Indices for IEEE RTS with 200 MW Wind Power Added at Different Buses: Data Set C

Wind Power at Bus No.	LOLP	EDNS (MW/y)	LOLF (f/y)	MDT (h)
1	0.001188	0.151188	2.171	4.79364
2	0.001207	0.153582	2.205	4.79410
3	0.001252	0.159732	2.261	4.84918
4	0.001262	0.160989	2.272	4.86576
5	0.001290	0.164816	2.311	4.89139
6	0.001115	0.140846	2.047	4.77040
7	0.001525	0.199972	2.657	5.02747
8	0.001359	0.174072	2.468	4.82253
9	0.001170	0.148830	2.138	4.79373
10	0.001152	0.146509	2.117	4.76665
13	0.001080	0.135374	1.969	4.80599
14	0.001306	0.167412	2.351	4.86729
15	0.001337	0.171378	2.413	4.85454
16	0.001136	0.144221	2.091	4.75849
18	0.001067	0.133227	1.940	4.81907
19	0.001160	0.147665	2.121	4.79208
20	0.001370	0.175437	2.491	4.81614

6.3.2 Storage System Augmentation for Different Wind Data Sets

The size of the energy storage P_{ESS} and the time t_S are calculated as explained in Section 6.1. A prediction error of $\gamma = 5\%$ is assumed for the annual energy production of the wind farm. The unavailability reduction ratio α is determined for each instance in the following manner. The wind farm is replaced by a conventional unit with the same nameplate capacity as the wind farm, i.e., 200 MW. Typical reliability characteristics are assumed for the conventional unit. Then, the system LOLP is calculated using the conventional unit instead of the wind farm, at the same location. This LOLP is deemed the target LOLP, since it is intended to use storage to firm the wind supply by increasing its reliability to the same level as that of a conventional unit. Now α is determined by dividing the target LOLP by the LOLP obtained from wind injection.

Then, the energy storage system is added to the grid at the candidate buses in presence of wind power. The storage system is sized as described in section 6.1.1. The power capacities P_{ESS} of the storage systems for data sets A, B and C are found to be 153.3 MW, 150.15 MW and 157.5 MW; these values differ because a higher positive correlation between wind and load requires a lower P_{ESS}. Then using α as calculated above, t_A is determined as described in section 6.1.1. The storage system is assumed to have 0.99 availability. From t_A and $A_S = 0.99$, t_S can be determined. But since the simulation is performed in hourly increments, t_S is rounded of to the nearest hour. The energy capacity of the storage system is given by $P_{ESS}t_S$.

The charging and discharging efficiencies of the storage are assumed 90% and 87.5% respectively [70]. During the simulation, the storage system logic described in section 6.1.2 is implemented. For the three case studies, the P_{ESS}, target LOLP, α, t_S, and the LOLP achieved with storage integration at each of the five selected locations are shown in Tables 6.4, 6.5 and 6.6.

Table 6.4 System Reliability Indices for IEEE RTS with Wind Power and Energy Storage at Different Buses: Data Set A

Wind Power at Bus No.	Target LOLP	P_{ESS} (MW)	α	t_S (h)	LOLP with Storage
18	0.00036	153.3	0.38	4	0.0003726
13	0.00039	153.3	0.41	4	0.0003808
6	0.00044	153.3	0.45	3	0.0004153
10	0.00053	153.3	0.52	3	0.0005445
9	0.00057	153.3	0.55	3	0.0005845

Table 6.5 System Reliability Indices for IEEE-RTS with Wind Power and Energy Storage at Different Buses: Data Set B

Wind Power at Bus No.	Target LOLP	P_{ESS} (MW)	α	t_S (h)	LOLP with Storage
18	0.00036	150.15	0.41	6	0.0003434
13	0.00039	150.15	0.43	5	0.0003856
6	0.00044	150.15	0.48	4	0.0004208
10	0.00053	150.15	0.56	3	0.0005217
9	0.00057	150.15	0.59	3	0.0005369

Table 6.6 System Reliability Indices for IEEE RTS with Wind Power and Energy Storage at Different Buses: Data Set C

Wind Power at Bus No.	Target LOLP	P_{ESS} (MW)	α	t_S (h)	LOLP with Storage
18	0.00036	157.5	0.34	8	0.0003686
13	0.00039	157.5	0.36	6	0.0004154
6	0.00044	157.5	0.40	6	0.0004300
10	0.00053	157.5	0.46	5	0.0005922
9	0.00057	157.5	0.49	4	0.0005836

As evident from Tables 6.4, 6.5 and 6.6, the proposed method was effective in firming the reliability of the wind farm using appropriate amounts of storage. The LOLP with storage was improved to the target LOLP, i.e., the same level as that of a conventional unit with the same nameplate capacity as the wind farm. It is also evident from these results how the storage capacity, both in MW and MWh, differ based on factors such as correlation between wind speed and load, and grid access, i.e., strength of interconnection to the grid. The results shown also validate the proposed methodology.

Chapter 7

Conclusions

This chapter summaries the findings and provides a general conclusion about the methods that have been developed in this work.

7.1 Conclusion

This work presented an analytical method of constructing reliability models of VERs for planning studies involving wind and PV system integration. The proposed method uses a recursive technique to build a generation model that considers input variability, correlation between VERs outputs, and forced outages of VERS. An illustrative reliability model was constructed using real input data and real. The effectiveness of the proposed method was demonstrated on a well-known test system. A comparison of several reliability indices (LOLP, LOLF, EDNS, LOLE and LOEE), with and without consideration of VER forced outages was provided in each case. The results obtained by the proposed method were validated using Monte Carlo simulation. The work presented here focused on the development of the reliability model of wind farms and PV systems; it did not attempt to capture correlations with other stochastic elements such as system load, for reasons described in section 4.2.1.3. The results of the case studies indicate that in the case of wind power, neglecting this correlation introduces small errors in some cases, but the advantages of an accurate and reusable model that can be used in analytical methods of adequacy assessment or capacity valuation may overshadow these errors. In applications where it is deemed necessary to consider such correlation, the approach described in [100] may be used. However, for the purpose of constructing an accurate reliability model of a wind farm and PV system, the proposed method was shown to be effective.

Further, this work has introduced a direct method to calculate the capacity value of VERs without performing iterations. The proposed method is based on augmenting the generation reserve margin to include the output power of VERs. The intermittency of wind, forced outages of WTGs, and correlation between WTGs on the farm were all considered. The proposed method was applied on IEEE RTS and the results provided. The proposed method reduces modeling complexity and the computational burden associated with calculating the capacity value of VERs using iterative methods. Capacity values estimated using an iterative method corroborated those obtained from the proposed method, thereby validating the method.

Also, a method for quantifying the amount of energy storage required to firm up wind power is presented in this work. Several case studies were performed to evaluate the reliability indices and determine the sizes and locations of the energy storage systems. Preferred locations for wind injection were also evaluated by comparing the enhancement of system reliability indices at the candidate buses. Sequential Monte Carlo simulation was used to emulate the stochastic behavior of wind power and forced outages of WTGs in calculating the reliability indices and determining the sizes of energy storage systems. In this work, three wind speed data sets were used. These data sets were utilized to study the effect of correlation between load demand and wind power, and of temporal resolutions on determining the size of the energy storage. The system reliability indices and the rated power of the energy storage systems were calculated for three case studies using the three data sets. These case studies were not intended to compare the results; they only demonstrate the effect of wind speed temporal resolution and correlation with the load on system reliability and determining size of the energy storage system. The results validated the proposed methodology and illustrated the dependence of the required sizes of storage systems on wind characteristics and wind farm location. Although the IEEE-RTS is considered a highly reliable system, some transmission lines have limited capacities. Therefore, placing wind farms at some buses may not improve system reliability. For example, placing a wind farm at bus 7 would not enhance the reliability of the system because the line connecting bus 7 with the rest of the grid cannot carry the available power due to the line capacity limit. On the other hand, other buses such as 13, 19, and 18 are connected with more than one transmission line to the system and they have higher loads compared to other load buses. In this regard, the reliability indices of the system are compared for different locations of wind farms and energy storage systems. These indices are dependent upon wind farm and energy storage system characteristics, as well as the connectivity with the rest of the system. These observations also indicate the importance of considering the influence of wind speed measurement resolutions and correlation with the load in evaluating the size of energy storage in planning projects. System reliability indices before and after installing the energy storage are also evaluated. From the EDNS indices it appears that bus 18 is the best location to site the wind farm.

7.2 Future Work

The work developed in this thesis could be extended further considering the following points:

1. The method presented in chapter 4 can be extended to construct a unified outage model of a clustered output of variable resources.

2. The method presented in chapter 5 is intended to calculate the capacity value of VERs in generation adequacy assessment utilizing a discrete convolution method. However, the method can be extended further for composite systems as well.

3. Because of the ongoing changes in generation portfolios, the integration of energy storage systems has become an important part in power system as it plays a major role in overcoming the challenges posed by the integration of variable resources. The method presented in this work can be extended to model both variable resources and energy storage systems in power system adequacy assessment.

4. One of the most important factors in power system planning projects is the evaluation of variable resources penetration levels. The method presented in chapter 5 can also be used to determine the optimal penetration levels of VERs.

BIBLIOGRAPHY

BIBLIOGRAPHY

[1] K. Fischer, F. Besnard, and L. Bertling, "Reliability-centered maintenance for wind turbines based on statistical analysis and practical experience," *IEEE Trans. Energy Convers.*, vol. 27, no. 1, pp. 184–195, 2012.

[2] R. M. Brandão, J. B. Carvalho, and F. M. Barbosa, "Forced outage time analysis of a portuguese wind farm," in *Universities Power Engineering Conference (UPEC), 2009 Proceedings of the 44th International.* IEEE, 2009, pp. 1–4.

[3] J. Ribrant and L. Bertling, "Survey of failures in wind power systems with focus on swedish wind power plants during 1997-2005," in *Power Engineering Society General Meeting.* IEEE, 2007, pp. 1–8.

[4] D. Hirschmann, D. Tissen, S. Schroder, and R. W. De Doncker, "Reliability prediction for inverters in hybrid electrical vehicles," *IEEE Trans. Power Electron.*, vol. 22, no. 6, pp. 2511–2517, 2007.

[5] G. Chen, R. Burgos, Z. Liang, F. Lacaux, F. Wang, J. D. van W. y. k., W. G. Odendaal, and D. Boroyevich, "Reliability-oriented design considerations for high-power converter modules," in *Proc. Power Electronics Specialists Conf.*, vol. 1. IEEE, 2004, pp. 419–425.

[6] U. De Pra, D. Baert, and H. Kuyken, "Analysis of the degree of reliability of a redundant modular inverter structure," in *INTELEC.* IEEE, 1998, pp. 23–1.

[7] H. Calleja, F. Chan, and I. Uribe, "Reliability-oriented assessment of a DC/DC converter for photovoltaic applications," in *Proc. Power Electronics Specialists Conf.* IEEE, 2007, pp. 1522–1527.

[8] F. Chan and H. Calleja, "Reliability estimation of three single-phase topologies in grid-connected PV systems," *IEEE Trans. Ind. Electron.*, vol. 58, no. 7, pp. 2683–2689, 2011.

[9] S. Persaud, B. Fox, and D. Flynn, "Modelling the impact of wind power fluctuations on the load following capability of an isolated thermal power system," *Wind Engineering*, vol. 24, no. 6, pp. 399–415, 2000.

[10] Y. Makarov, J. Blatchford, H. Alarian, K. DeMarse, M. OHara, M. Scholz, S. Jercich, J. Vidov, E. Leuze, R. Abernathy *et al.*, "Incorporation of wind power resources into

the california energy market," in *Proc. Wind power Conf. Exhib.* Citeseer, 2005, pp. 15–18.

[11] J. C. Smith, M. R. Milligan, E. A. DeMeo, and B. Parsons, "Utility wind integration and operating impact state of the art," *IEEE Trans. Power Syst.*, vol. 22, no. 3, pp. 900–908, 2007.

[12] D. Brooks, E. Lo, R. Zavadil, S. Santoso, and J. Smith, "Characterizing the impacts of significant wind generation facilities on bulk power system operation planning," *prepared for Utility Wind Integration Group, Arlington, VA*, 2003.

[13] L. Soder, L. Hofmann, A. Orths, H. Holttinen, Y.-h. Wan, and A. Tuohy, "Experience from wind integration in some high penetration areas," *IEEE Trans. Energy Convers.*, vol. 22, no. 1, pp. 4–12, 2007.

[14] H. Kim, C. Singh, and A. Sprintson, "Simulation and Estimation of Reliability in a Wind Farm Considering the Wake Effect," *IEEE Trans. Sustain. Energy*, vol. 3, no. 2, pp. 274–282, Apr. 2012.

[15] C. Singh and A. Lago-Gonzalez, "Reliability modeling of generation systems including unconventional energy sources," *IEEE Trans. Power App. Syst.*, no. 5, pp. 1049–1056, 1985.

[16] C. Singh and Y. Kim, "An Efficient Technique for Reliability Analysis of Power Systems Including Time Dependent Sources," *IEEE Trans. Power Syst.*, vol. 3, no. 3, pp. 1090–1096, Aug. 1988.

[17] P. Giorsetto and K. F. Utsurogi, "Development of a new procedure for reliability modeling of wind turbine generators," *IEEE Trans. Power App. Syst.*, no. 1, pp. 134–143, 1983.

[18] F. C. Sayas and R. Allan, "Generation availability assessment of wind farms," in *Generation, Transmission and Distribution, IEE Proceedings-*, vol. 143, no. 5. IET, 1996, pp. 507–518.

[19] A. P. Leite, C. L. Borges, and D. M. Falcao, "Probabilistic wind farms generation model for reliability studies applied to brazilian sites," *IEEE Trans. Power Syst.*, vol. 21, no. 4, pp. 1493–1501, 2006.

[20] A. R. Di Fazio and M. Russo, "Wind farm modelling for reliability assessment," *Renewable Power Generation, IET*, vol. 2, no. 4, pp. 239–248, 2008.

[21] J. Lin, L. Cheng, Y. Chang, K. Zhang, B. Shu, and G. Liu, "Reliability based power systems planning and operation with wind power integration: A review to models, algorithms and applications," *Renewable and Sustain. Energy Reviews*, vol. 31, pp. 921–934, 2014.

[22] F. Vallee, J. Lobry, and O. Deblecker, "System reliability assessment method for wind power integration," *IEEE Trans. Power Syst.*, vol. 23, no. 3, pp. 1288–1297, 2008.

[23] R. Billinton, H. Chen, and R. Ghajar, "A sequential simulation technique for adequacy evaluation of generating systems including wind energy," *IEEE Trans. Energy Convers.*, vol. 11, no. 4, pp. 728–734, 1996.

[24] G. Papaefthymiou and B. Klockl, "Mcmc for wind power simulation," *IEEE Trans. Energy Convers.*, vol. 23, no. 1, pp. 234–240, 2008.

[25] Y. Hegazy, M. Salama, and A. Chikhani, "Adequacy assessment of distributed generation systems using monte carlo simulation," *IEEE Trans. Power Syst.*, vol. 18, no. 1, pp. 48–52, 2003.

[26] A. Chen, L. Hu, L. Chen, Y. Deng, and X. He, "A multilevel converter topology with fault-tolerant ability," *IEEE Trans. Power Electron.*, vol. 20, no. 2, pp. 405–415, 2005.

[27] L. N. Dumas and A. Shumka, "Photovoltaic module reliability improvement through application testing and failure analysis," *IEEE Trans. Rel.*, vol. 31, no. 3, pp. 228–234, 1982.

[28] E. L. Meyer and E. Ernest van Dyk, "Assessing the reliability and degradation of photovoltaic module performance parameters," *IEEE Trans. Rel.*, vol. 53, no. 1, pp. 83–92, 2004.

[29] P. Zhang, W. Li, S. Li, Y. Wang, and W. Xiao, "Reliability assessment of photovoltaic power systems: Review of current status and future perspectives," *Applied Energy*, vol. 104, pp. 822–833, 2013.

[30] A. H. Fanney, M. W. Davis, B. P. Dougherty, D. L. King, W. E. Boyson, and J. A. Kratochvil, "Comparison of photovoltaic module performance measurements," *Journal of Solar Energy Engineering*, vol. 128, no. 2, pp. 152–159, 2006.

[31] Y. Song and B. Wang, "Survey on reliability of power electronic systems," *IEEE Trans. Power Electron.*, vol. 28, no. 1, pp. 591–604, 2013.

[32] B. Abdi, A. H. Ranjbar, G. B. Gharehpetian, and J. Milimonfared, "Reliability considerations for parallel performance of semiconductor switches in high-power switching power supplies," *Industrial Electronics, IEEE Transactions on*, vol. 56, no. 6, pp. 2133–2139, 2009.

[33] G. Chen, R. Burgos, Z. Liang, F. Lacaux, F. Wang, J. D. van Wyk, W. G. Odendaal, and D. Boroyevich, "Reliability-oriented design considerations for high-power converter modules," in *Proc. Power 35th Annual Electronics Specialists Conf.*, vol. 1. IEEE, 2004, pp. 419–425.

[34] Y. Wang, P. Zhang, W. Li, and N. H. Kan'an, "Comparative analysis of the reliability of grid-connected photovoltaic power systems," in *Power and Energy Society General Meeting*. IEEE, 2012, pp. 1–8.

[35] L. M. Tolbert and F. Z. Peng, "Multilevel converters as a utility interface for renewable energy systems," in *Proc. Power Engineering Society Summer Meeting*, vol. 2. IEEE, 2000, pp. 1271–1274.

[36] M. Benidris, S. Elsaiah, and J. Mitra, "Sensitivity analysis of reliability performance of multi-level converters," in *Proc. North American Power Symposium*. IEEE, 2012, pp. 1–6.

[37] L. Kishore and E. Fernandez, "Reliability well-being assessment of pv-wind hybrid system using monte carlo simulation," in *Proc. International Conf. Emerging Trends in Electrical and Computer Technology (ICETECT)*. IEEE, 2011, pp. 63–68.

[38] R. M. Moharil and P. S. Kulkarni, "Reliability analysis of solar photovoltaic system using hourly mean solar radiation data," *Solar Energy*, vol. 84, no. 4, pp. 691–702, 2010.

[39] A. Ghaedi, A. Abbaspour, M. Fotuhi-Friuzabad, and M. Parvania, "Incorporating large photovoltaic farms in power generation system adequacy assessment," *J. Sci. Iran*, vol. 21, no. 3, pp. 924–934, 2014.

[40] N. Pradhan and N. R. Karki, "Probabilistic reliability evaluation of off-grid small hybrid solar PV-wind power system for the rural electrification in nepal," in *North American Power Symposium (NAPS), 2012*. IEEE, 2012, pp. 1–6.

[41] L. H. Stember, W. R. Huss, and M. S. Bridgman, "A methodology for photovoltaic system reliability & economic analysis," *IEEE Trans. Rel.*, vol. 31, no. 3, pp. 296–303, 1982.

[42] S. E. Forman, "Performance of experimental terrestrial photovoltaic modules," *IEEE Trans. on Rel.*, vol. 31, no. 3, pp. 235–245, 1982.

[43] A. H. Fanney, M. W. Davis, B. P. Dougherty, D. L. King, W. E. Boyson, and J. A. Kratochvil, "Comparison of photovoltaic module performance measurements," *Journal of solar energy engineering*, vol. 128, no. 2, pp. 152–159, 2006.

[44] R. M. Castro and L. Ferreira, "A comparison between chronological and probabilistic methods to estimate wind power capacity credit," *IEEE Trans. Power Syst.*, vol. 16, no. 4, pp. 904–909, 2001.

[45] M. Amelin, "Comparison of capacity credit calculation methods for conventional power plants and wind power," *IEEE Trans. Power Syst.*, vol. 24, no. 2, pp. 685–691, 2009.

[46] S. H. Madaeni, R. Sioshansi, and P. Denholm, "Comparing capacity value estimation techniques for photovoltaic solar power," *IEEE J. Photovolt.*, vol. 3, no. 1, pp. 407–415, Jan 2013.

[47] S. H. Madaeni, R. Sioshansi, and P. Denholm, "Estimating the capacity value of concentrating solar power plants: A case study of the southwestern united states," *IEEE Trans. Power Syst.*, vol. 27, no. 2, pp. 1116–1124, 2012.

[48] L. Wang and C. Singh, "An Alternative Method for Estimating Wind-Power Capacity Credit based on Reliability Evaluation Using Intelligent Search," in *Proc. of the 10th International Conference on Probabilistic Methods Applied to Power Systems*, Mayagez, Puerto Rico, May 2008, pp. 1–6.

[49] R. Billinton and Hua Chen, "Assessment of risk-based capacity benefit factors associated with wind energy conversion systems," *IEEE Trans. Power Syst.*, vol. 13, no. 3, pp. 1191–1196, Aug. 1998.

[50] W. Wangdee and R. Billinton, "Considering load-carrying capability and wind speed correlation of wecs in generation adequacy assessment," *IEEE Trans. Energy Convers.*, vol. 21, no. 3, pp. 734–741, 2006.

[51] G. R. Pudaruth and F. Li, "Locational Capacity Credit Evaluation," *IEEE Trans. Power Syst.*, vol. 24, no. 2, pp. 1072–1079, May 2009.

[52] Z. Chen, L. Wu and M. Shahidehpour, "Effective load carrying capability evaluation of renewable energy via stochastic long-term hourly based scuc," *IEEE Trans. Sust. Energy*, vol. 6, no. 1, pp. 188–197, Jan. 2015.

[53] M. Mosadeghy, R. Yan, and T. K. Saha, "A time-dependent approach to evaluate capacity value of wind and solar pv generation," *IEEE Trans. Sust. Energy*, vol. 7, no. 1, pp. 129–138, Jan. 2016.

[54] S. Sulaeman, M. Benidris, and J. Mitra, "Evaluation of wind power capacity value including effects of transmission system," in *Proc. of North American Power Symposium*, Charlotte, NC, USA, Oct. 2015, pp. 1–6.

[55] S. Zhang, G. Li, and M. Zhou, "Calculation and analysis of capacity credit of wind farms based on monte-carlo simulation," in *Proc. IEEE PES General Meeting.* IEEE, 25-29 July 2010, pp. 1–6.

[56] A. M. Leite da Silva, R. A. G. Fernndez, and C. Singh, "Generating capacity reliability evaluation based on monte carlo simulation and cross-entropy methods," *IEEE Trans. Power Syst.*, vol. 25, no. 1, pp. 129–137, 2010.

[57] R. M. Moharil and P. S. Kulkarni, "Reliability analysis of solar photovoltaic system using hourly mean solar radiation data," *Solar Energy*, vol. 84, no. 4, pp. 691–702, 2010.

[58] B. Hasche, A. Keane, and M. O'Malley, "Capacity Value of Wind Power, Calculation, and Data Requirements: the Irish Power System Case," *IEEE Trans. Power Syst.*, vol. 26, no. 1, pp. 420–430, Feb. 2011.

[59] A. Keane, M. Milligan, C. J. Dent, B. Hasche, C. D'Annunzio, K. Dragoon, H. Holttinen, N. Samaan, L. Soder, and M. O'Malley, "Capacity Value of Wind Power," *IEEE Trans. Power Syst*, vol. 26, no. 2, pp. 564–572, May 2011.

[60] S. Sulaeman, M. Benidris, and J. Mitra, "Evaluation of Wind Capacity Credit Using Discrete Convolution Considering the Mechanical Failure of Wind Turbines," in *Proc. of 13th International Conference on Probabilistic Methods Applied to Power Systems*, Durham, United Kingdom, July 2014, pp. 1–6.

[61] C. D'Annunzio and S. Santoso, "Noniterative Method to Approximate the Effective Load Carrying Capability of a Wind Plant," *IEEE Trans. Energy Convers.*, vol. 23, no. 2, pp. 544–550, June 2008.

[62] K. Dragoon and V. Dvortsov, "Z-Method for Power System Resource Adequacy Applications," *IEEE Trans. Power Syst.*, vol. 21, no. 2, pp. 982–988, May 2006.

[63] M. A. Abdullah, K. M. Muttaqi, A. P. Agalgaonkar, and D. Sutanto, "A Noniterative Method to Estimate Load Carrying Capability of Generating Units in a Renewable

Energy Rich Power Grid," *IEEE Trans. Sust. Energy*, vol. 5, no. 3, pp. 854–865, July 2014.

[64] L. Garver, "Effective load carrying capability of generating units," *IEEE Trans. Power App. Syst.*, vol. 8, no. PAS-85, pp. 910–919, 1966.

[65] C. J. Dent and A. Keane and J. W. Bialek, "Simplified methods for renewable generation capacity credit calculation: a critical review," in *IEEE PES General Meeting*. IEEE, 25–29 July 2010, pp. 1–8.

[66] F. C. Figueiredo, P. C. Flynn, and E. A. Cabral, "The economics of energy storage in 14 deregulated power markets," *Energy Studies Review*, vol. 14, no. 2, p. 131, 2006.

[67] S. Schoenung and J. Eyer, "Benefit and cost comparison of energy storage technologies for three emerging value propositions," 2005. [Online]. Available: http://www.sandia.gov/ess/docs/pr_conferences/2005/Schoenung.pdf

[68] D. W. Sobieski and M. P. Bhavaraju, "An economic assessment of battery storage in electric utility systems," *IEEE Trans. Power App. Syst.*, vol. PAS-104, no. 12, pp. 3453–3459, Dec. 1985.

[69] C. H. Lo and M. D. Anderson, "Economic dispatch and optimal sizing of battery energy storage systems in utility load-leveling operations," *IEEE Trans. Energy Convers.*, vol. 14, no. 3, pp. 824–829, 1999.

[70] P. Xiong and C. Singh, "Optimal planning of storage in power systems integrated with wind power generation," *IEEE Trans. Sustain. Energy*, vol. 7, no. 1, pp. 232–240, 2016.

[71] B. Dunn, H. Kamath, and J.-M. Tarascon, "Electrical energy storage for the grid: a battery of choices," *Science*, vol. 334, no. 6058, pp. 928–935, 2011.

[72] J. Eyer and G. Corey, "Energy storage for the electricity grid: Benefits and market potential assessment guide," *Sandia National Laboratories*, vol. 20, no. 10, p. 5, 2010.

[73] C. Abbey and G. Joós, "A stochastic optimization approach to rating of energy storage systems in wind-diesel isolated grids," *IEEE Trans. Power Syst.*, vol. 24, no. 1, pp. 418–426, 2009.

[74] P. Pinson, G. Papaefthymiou, B. Klockl, and J. Verboomen, "Dynamic sizing of energy storage for hedging wind power forecast uncertainty," in *Proc. IEEE Power & Energy Soc. General Meeting*. IEEE, 2009, pp. 1–8.

[75] X. Y. Wang, D. M. Vilathgamuwa, and S. S. Choi, "Determination of battery storage capacity in energy buffer for wind farm," *IEEE Trans. Energy Convers.*, vol. 23, no. 3, pp. 868–878, 2008.

[76] C.-T. Li, H. Peng, and J. Sun, "MPC for reducing energy storage requirement of wind power systems," in *Proc. American Control Conference*. IEEE, 2013, pp. 6607–6612.

[77] C. H. Lo and M. D. Anderson, "Economic dispatch and optimal sizing of battery energy storage systems in utility load-leveling operations," *IEEE Trans. Energy Convers.*, vol. 14, no. 3, pp. 824–829, 1999.

[78] F. A. Chacra, P. Bastard, G. Fleury, and R. Clavreul, "Impact of energy storage costs on economical performance in a distribution substation," *IEEE Trans. Power Syst*, vol. 20, no. 2, pp. 684–691, 2005.

[79] K. C. Divya and J. Østergaard, "Battery energy storage technology for power systemsan overview," *Electric Power Syst. Research*, vol. 79, no. 4, pp. 511–520, 2009.

[80] S. Persaud, B. Fox, and D. Flynn, "Modelling the impact of wind power fluctuations on the load following capability of an isolated thermal power system," *Wind Engineering*, vol. 24, no. 6, pp. 399–415, 2000.

[81] S. Sulaeman, M. Benidris, J. Mitra, and C. Singh, "A wind farm reliability model considering both wind variability and turbine forced outages," *IEEE Trans. Sustain. Energy*, vol. PP, no. 99, pp. 1–9, Sept. 2016.

[82] L. Lin and S. Wang, "Investigation of the strategy of wind farm power regulation considering system frequency regulation demand," in *Proc. 4th Int. Conf. on Elect. utility deregulation and restructuring and power technologies (DRPT)*, July 2011, pp. 1138–1143.

[83] M. M. Daniel L. Brooks, John H. Pease. (2002) Assessing the impact of wind generation on system operations at xcel energy-north and bonneville power administration. [Online]. Available: https://pdfs.semanticscholar.org/0ec3/77325e69197b635a890e256e105d723179af.pdf

[84] J. Cadogan, M. Milligan, Y. Wan, and B. Kirby, "Short-term output variations in wind farms-implications for ancillary services in the united states," *Wind Power for the 21st Century, Kassel, Germany*, 2000.

[85] S. Sulaeman, Y. Tian, M. Benidris, and J. Mitra, "Quantification of storage necessary to firm up wind generation," in *Proc. Ind. Applicat. Soc. Annu. Meeting.* IEEE, 2016, pp. 1–7.

[86] X. Luo, J. Wang, M. Dooner, and J. Clarke, "Overview of current development in electrical energy storage technologies and the application potential in power system operation," *Applied Energy*, vol. 137, pp. 511–536, 2015.

[87] Lazard. (2015) Lazard's levelized cost of storage analysis. [Online]. Available: https://www.lazard.com/media/2393/lazard-s-levelized-cost-of-storage-analysis-10-key-findings.pdf

[88] S. Schoenung. (2011) Energy storage systems cost update: A study for the DOE energy storage systems program (report sand2011-2730). [Online]. Available: http://prod.sandia.gov/techlib/access-control.cgi/2011/112730.pdf

[89] J. Mitra, "Reliability-based sizing of backup storage," *IEEE Trans. Power Syst.*, vol. 25, no. 2, pp. 1198–1199, 2010.

[90] J. Mitra and M. R. Vallem, "Determination of storage required to meet reliability guarantees on island-capable microgrids with intermittent sources," *IEEE Trans. Power Syst.*, vol. 27, no. 4, pp. 2360–2367, 2012.

[91] R. N. Allan *et al.*, *Reliability evaluation of power systems.* Springer Science & Business Media, 2013.

[92] R. Billinton and R. N. Allan, *Reliability assessment of large electric power systems.* Springer Science & Business Media, 2012.

[93] J. Mitra, "Power system reliability and risk assessment-lecture class notes," *Michigan State University.*

[94] R. Billinton, C. Wee, and G. Hamoud, "Digital computer algorithms for the calculation of generating capacity reliability indices," *Power Engineering Review, IEEE*, no. 1, pp. 34–35, 1982.

[95] R. Billinton and C. Singh, "Generating capacity reliability evaluation in interconnected systems using a frequency and duration approach part i. mathematical analysis," *IEEE Trans. Power App. Syst.*, vol. PAS-90, no. 4, pp. 1646–1654, July 1971.

[96] A. M. Leite da Silva, R. A. Fernandez, and C. Singh, "Generating capacity reliability evaluation based on monte carlo simulation and cross-entropy methods," *IEEE Trans. Power Syst.*, vol. 25, no. 1, pp. 129–137, 2010.

[97] R. Billinton and P. Wang, "Teaching distribution system reliability evaluation using monte carlo simulation," *IEEE Trans. Power Syst.*, vol. 14, no. 2, pp. 397–403, 1999.

[98] R. Billinton, C. Wee, and G. Hamoud, "Digital computer algorithms for the calculation of generating capacity reliability indices," *Power Engineering Review, IEEE*, no. 1, pp. 34–35, 1982.

[99] C. Singh and Q. Chen, "Generation system reliability evaluation using a cluster based load model," *IEEE Trans. Power Syst.*, vol. 4, no. 1, pp. 102–107, 1989.

[100] R. Billinton and D. Huang, "Incorporating wind power in generating capacity reliability evaluation using different models," *IEEE Trans power syst.*, vol. 26, no. 4, pp. 2509–2517, 2011.

[101] R. Billinton, H. Chen, and R. Ghajar, "Time-series models for reliability evaluation of power systems including wind energy," *Microelectronics Reliability*, vol. 36, no. 9, pp. 1253–1261, 1996.

[102] J. F. Manwell, J. G. McGowan, and A. L. Rogers, *Wind energy explained: theory, design and application.* John Wiley & Sons, 2010.

[103] J. Ge, M. Du, and C. Zhang, "A study on correlation of wind farms output in the large-scale wind power base," in *Proc. 4th International Conf. Electric Utility Deregulation and Restructuring and Power Technologies.* IEEE, 2011, pp. 1316–1319.

[104] H. Holttinen, "Impact of hourly wind power variations on the system operation in the nordic countries," *Wind Energy*, vol. 8, no. 2, pp. 197–218, 2005.

[105] B. Hasche, "General statistics of geographically dispersed wind power," *Wind Energy*, vol. 13, no. 8, pp. 773–784, 2010.

[106] B. Ernst, Y.-H. Wan, and B. Kirby, "Short-term power fluctuation of wind turbines: analyzing data from the german 250-mw measurement program from the ancillary services viewpoint," in *WindPower '99 Conference*, Burlington, Vermont, June 20–23, 1999, pp. 1–10.

[107] Y.-h. Wan, M. Milligan, and B. Parsons, "Output power correlation between adjacent wind power plants," *Journal of Solar Energy Engineering*, vol. 125, no. 4, pp. 551–555, 2003.

[108] H. Louie, "Correlation and statistical characteristics of aggregate wind power in large transcontinental systems," *Wind Energy*, vol. 17, no. 6, pp. 793–810, 2014.

[109] T. Nanahara, M. Asari, T. Maejima, T. Sato, K. Yamaguchi, and M. Shibata, "Smoothing effects of distributed wind turbines. part 2. coherence among power output of distant wind turbines," *Wind Energy*, vol. 7, no. 2, pp. 75–85, 2004.

[110] P. Kádár, "Evaluation of correlation the wind speed measurements and wind turbine characteristics," in *in 8th International Symposium of Hungarian Researchers on Computational Intelligence and Informatics, CINTI*, vol. 2007, 2007, pp. 15–17.

[111] J. Ubeda and M. Rodriguez Garcia, "Reliability and production assessment of wind energy production connected to the electric network supply," in *Generation, Transmission and Distribution, IEE Proceedings-*, vol. 146, no. 2. IET, 1999, pp. 169–175.

[112] H. Sipeng, Z. Yangfei, L. Xianyun, and Y. Yue, "Equivalent wind speed model in wind farm dynamic analysis," in *Electric Utility Deregulation and Restructuring and Power Technologies (DRPT), 2011 4th International Conference on*. IEEE, 2011, pp. 1751–1755.

[113] sirisha tanneeru, "Reliability modeling of dg clusters," diploma thesis, New Mexico State University, unites state, 2008.

[114] S. Venkatraman *et al.*, "Integration of renewable resources," California ISO, Folsom, CA, Tech. Rep., August 2010.

[115] K. Coughlin and J. H. Eto, "Analysis of wind power and load data at multiple time scales," Technical Report LBNL-4147E, U.S. Department of Energy, Washington, DC, USA, Tech. Rep., 2010.

[116] B. Martin and J. Carlin, "Wind-load correlation and estimates of the capacity credit of wind power: An empirical investigation," *Wind Engineering*, vol. 7, no. 2, p. 79, 1983.

[117] C. Singh and Q. Chen, "Generation system reliability evaluation using a cluster based load model," *IEEE Trans. Power Syst.*, vol. 4, no. 1, pp. 102–107, 1989.

[118] K. Fischer, F. Besnard, and L. Bertling, "Reliability-centered maintenance for wind turbines based on statistical analysis and practical experience," *IEEE Trans. Energy Convers.*, vol. 27, no. 1, pp. 184–195, 2012.

[119] J. Ribrant and L. Bertling, "Survey of failures in wind power systems with focus on swedish wind power plants during 1997-2005," in *Power Engineering Society General Meeting*. IEEE, 2007, pp. 1–8.

[120] F. Spinato, P. Tavner, G. Van Bussel, and E. Koutoulakos, "Reliability of wind turbine subassemblies," *IET Renewable Power Generation*, vol. 3, no. 4, pp. 387–401, 2009.

[121] H. Guo, S. Watson, P. Tavner, and J. Xiang, "Reliability analysis for wind turbines with incomplete failure data collected from after the date of initial installation," *Reliability Engineering & System Safety*, vol. 94, no. 6, pp. 1057–1063, 2009.

[122] Y. Feng, P. J. Tavner, and H. Long, "Early experiences with uk round 1 offshore wind farms," *Proceedings of the ICE-Energy*, vol. 163, no. 4, pp. 167–181, 2010.

[123] R. T. Force, "The ieee reliability test system-1996," *IEEE Trans. Power Syst*, vol. 14, no. 3, pp. 1010–1020, 1999.

[124] V. products and services. (2015). [Online]. Available: http://www.vestas.com/en/products_and_services_turbines\\/v90_3_mw_technical-specifications.

[125] F. Spinato, P. J. Tavner, G. J. W. V. Bussel, and E. Koutoulakos, "Reliability of Wind Turbine Subassemblies," *IET Renewable Power Generation*, vol. 3, no. 4, pp. 387–401, December 2009.

[126] N. climate data and information archive. (2007) Bonavista newfoundland, canada. [Online]. Available: http://www.climate.weatherofce.gc.ca/climateData/canada_e.html.

[127] G. d. National renewable energy laboratory (NREL), dynamic maps and analysis tools.

[128] Great Lakes Environmental Research Laboratory. (2005). [Online]. Available: http://www.glerl.noaa.gov/metdata/mil/archive/mil2005.01t.txt

[129] R. Carbone and A. Tomaselli, "Recent advances on AC PV-modules for grid-connected photovoltaic plants," in *Proc. International Conf. on Clean Electrical Power (ICCEP)*. IEEE, 2011, pp. 124–129.

[130] D. Picault, B. Raison, and S. Bacha, "Guidelines for evaluating grid connected pv system topologies," in *Proc. International Conf. Industrial Technology.* IEEE, 2009, pp. 1–5.

[131] S. Forman, "Performance of experimental terrestrial photovoltaic modules," *IEEE Trans. Rel.*, vol. 31, no. 3, pp. 235–245, 1982.

[132] P. Zhang, W. Li, S. Li, Y. Wang, and W. Xiao, "Reliability assessment of photovoltaic power systems: review of current status and future perspectives," *Applied Energy*, vol. 104, pp. 822–833, 2013.

[133] D. K. Khatod, V. Pant, and J. Sharma, "Analytical approach for well-being assessment of small autonomous power systems with solar and wind energy sources," *IEEE Trans. Energy Convers.*, vol. 25, no. 2, pp. 535–545, 2010.

[134] C. R. S. Reinoso, D. H. Milone, and R. H. Buitrago, "Simulation of photovoltaic centrals with dynamic shading," *Applied Energy*, vol. 103, pp. 278–289, 2013.

[135] U. De Pra, D. Baert, and H. Kuyken, "Analysis of the degree of reliability of a redundant modular inverter structure," in *Twentieth International Telecommunications Energy Conference.* IEEE, 06 August 2002, pp. 543–548.

[136] M. Benidris, S. Elsaiah, and J. Mitra, "Sensitivity analysis of reliability performance of multi-level converters," in *Proc. North American Power Symposium (NAPS).* IEEE, 2012, pp. 1–6.

[137] R. Ramakumar, *Engineering reliability: fundamentals and applications.* Prentice Hall, 1993.

[138] ——, *Engineering reliability: fundamentals and applications.* Prentice Hall, 1993.

[139] U. SPECS, "Military handbook reliability prediction of electronic equipment, MIL-HDBK-217F," 1992.

[140] P. Subcommittee, "Ieee reliability test system," *IEEE Trans. Power App. Syst.*, pp. 2047–2054, 1979.

[141] A. Garro and F. Barrara, "Reliability analysis of residential photovoltaic systems," in *Proc. Int. Conf. Renewable Energies Power Quality*, vol. 11, 2011.

[142] G. R. Pudaruth and F. Li, "Capacity credit evaluation: A literature review," in *in Proc. Third International Conference Electric Utility Deregulation and Restructuring and Power Technologies*. IEEE, 2008, pp. 2719–2724.

[143] C. F. DeSieno and L. L. Stine, "A probability method for determining the reliability of electric power systems," *IEEE Trans. Power App. Syst*, vol. 83, no. 2, pp. 174–181, 1964.

[144] M. R. Milligan and B. K. Parsons, *A comparison and case study of capacity credit algorithms for intermittent generators*. National Renewable Energy Laboratory, 1997.

[145] C. Ensslin, M. Milligan, H. Holttinen, M. O'Malley, and A. Keane, "Current methods to calculate capacity credit of wind power, iea collaboration," in *Proc. Power and Energy Society General Meeting-Conversion and Delivery of Electrical Energy in the 21st Century*. IEEE, 2008, pp. 1–3.

[146] National Renewable Energy Laboratory. (2015). [Online]. Available: https://maps.nrel.gov/wind-prospector/

[147] X. Zhang and W. Wang, "Wind farm and wake effect modeling for simulation of a studied power system," in *Proc. IEEE Power Systems Conf. Exposition (PSCE)*. IEEE, 2009, pp. 1–6.

[148] J. F. Ainslie, "Calculating the flow field in the wake of wind turbines," *Journal of Wind Engineering and Industrial Aerodynamics*, vol. 27, no. 1, pp. 213–224, 1988.

[149] National Renewable Energy Laboratory. Golden, CO. (2016) System Advisor Model Version 2012.5.11 (SAM 2012.5.11). [Online]. Available: https://sam.nrel.gov

[150] M. A. Lackner, A. L. Rogers, and J. F. Manwell, "Uncertainty analysis in wind resource assessment and wind energy production estimation," in *Proc. 45th AIAA Aerospace Sciences Meeting and Exhibit*, 2007.

[151] ——, "Uncertainty analysis in mcp-based wind resource assessment and energy production estimation," *J. Solar Energy Eng.*, vol. 130, no. 3, p. 031006, 2008.

[152] C. Jaworsky, K. Turitsyn, and S. Backhaus, "The effect of forecasting accuracy on the sizing of energy storage," in *Proc. Dynamic Syst. and Control Conf.* American Society of Mechanical Engineers, 2014, pp. V002T22A005–V002T22A005.

[153] R.-N. Liao, T.-H. Chen, and W.-S. Chang, "Fast screening techniques and process for grid interconnection of wind-storage systems," *Energy*, vol. 115, pp. 770–780, 2016.

[154] M. A. Lackner, A. L. Rogers, and J. F. Manwell, "The round robin site assessment method: A new approach to wind energy site assessment," *Renewable Energy*, vol. 33, no. 9, pp. 2019–2026, 2008.

[155] R. Wiser, M. Bolinger *et al.* (2008) Wind technologies market report. [Online]. Available: http://www.nrel.gov/docs/fy09osti/46026.pdf

[156] Z. Shu, K. T. K. Hock, and G. H. Beng, "Operation of energy storage system for renewable utilization enhancement," in *Proc. Power and Energy Soc. General Meeting (PESGM)*. IEEE, 2016, pp. 1–5.

[157] R. Fernandez-Blanco, Y. Dvorkin, B. Xu, Y. Wang, and D. S. Kirschen, "Optimal energy storage siting and sizing: A WECC case study," *IEEE Trans. Sustain. Energy*, pp. 1–8, 2016.

[158] W. Li, *Risk Assessment of Power Systems.* USA, IEEE Press: Wiley-Interscience, 2005.

[159] W. Li *et al.*, *Reliability assessment of electrical power systems using Monte Carlo methods.* Springer Science & Business Media, 1994.

[160] Great Lakes Environmental Research Laboratory. (2005). [Online]. Available: http://www.glerl.noaa.gov/metdata/mil/archive/mil2005.01t.txt